

# Hammerhead flatworms (Platyhelminthes, Geoplanidae, Bipaliinae): mitochondrial genomes and description of two new species from France, Italy, and Mayotte

Jean-Lou Justine<sup>1</sup>, Romain Gastineau<sup>2</sup>, Pierre Gros<sup>3</sup>, Delphine Gey<sup>4</sup>, Enrico Ruzzier<sup>5</sup>, Laurent Charles<sup>6</sup> and Leigh Winsor<sup>7</sup>

<sup>1</sup> ISYEB-Institut de Systématique, Évolution, Biodiversité, Muséum National d'Histoire Naturelle, Paris, France

<sup>2</sup> Institute of Marine and Environmental Sciences, University of Szczecin, Szczecin, Poland

<sup>3</sup> Amateur Naturalist, Unaffiliated, Cagnes-sur-Mer, France

<sup>4</sup> Molécules de Communication et Adaptation des Micro-Organismes, Muséum National d'Histoire Naturelle, Paris, France

<sup>5</sup> Department of Agronomy, Food, Natural Resources, Animals and the Environment (DAFNAE), Padova, Italy

<sup>6</sup> Muséum de Bordeaux - science et nature, Bordeaux, France

<sup>7</sup> James Cook University, Townsville, Queensland, Australia

## ABSTRACT

**Background:** New records of alien land planarians are regularly reported worldwide, and some correspond to undescribed species of unknown geographic origin.

The description of new species of land planarians (Geoplanidae) should classically be based on both external morphology and histology of anatomical structures, especially the copulatory organs, ideally with the addition of molecular data.

**Methods:** Here, we describe the morphology and reproductive anatomy of a species previously reported as *Diversibipalium* “black”, and the morphology of a species previously reported as *Diversibipalium* “blue”. Based on next generation sequencing, we obtained the complete mitogenome of five species of Bipaliinae, including these two species.

**Results:** The new species *Humbertium covidum* n. sp. (syn: *Diversibipalium* “black” of Justine et al., 2018) is formally described on the basis of morphology, histology and mitogenome, and is assigned to *Humbertium* on the basis of its reproductive anatomy. The type-locality is Casier, Italy, and other localities are in the Department of Pyrénées-Atlantiques, France; some published or unpublished records suggest that this species might also be present in Russia, China, and Japan. The mitogenomic polymorphism of two geographically distinct specimens (Italy vs France) is described; the *cox1* gene displayed 2.25% difference. The new species *Diversibipalium mayottensis* n. sp. (syn: *Diversibipalium* “blue” of Justine et al., 2018) is formally described on the basis of external morphology and complete mitogenome and is assigned to *Diversibipalium* on the basis of an absence of information on its reproductive anatomy. The type- and only known locality is the island of Mayotte in the Mozambique Channel off Africa. Phylogenies of bipaliine geoplanids were constructed on the basis of SSU, LSU, mitochondrial proteins and concatenated sequences of *cox1*, SSU and LSU. In all four phylogenies, *D. mayottensis* was the sister-group to all the other bipaliines. With the exception of *D. multilineatum* which

Submitted 18 August 2021

Accepted 10 December 2021

Published 1 February 2022

Corresponding author

Jean-Lou Justine, justine@mnhn.fr

Academic editor

Marta Riutort

Additional Information and  
Declarations can be found on  
page 49

DOI 10.7717/peerj.12725

© Copyright

2022 Justine et al.

Distributed under

Creative Commons CC-BY 4.0

OPEN ACCESS

could not be circularised, the complete mitogenomes of *B. kewense*, *B. vagum*, *B. adventitium*, *H. covidum* and *D. mayottensis* were colinear. The 16S gene in all bipaliine species was problematic because usual tools were unable to locate its exact position.

**Conclusion:** Next generation sequencing, which can provide complete mitochondrial genomes as well as traditionally used genes such as SSU, LSU and *cox1*, is a powerful tool for delineating and describing species of Bipaliinae when the reproductive structure cannot be studied, which is sometimes the case of asexually reproducing invasive species. The unexpected position of the new species *D. mayottensis* as sister-group to all other Bipaliinae in all phylogenetic analyses suggests that the species could belong to a new genus, yet to be described.

**Subjects** Biodiversity, Conservation Biology, Taxonomy, Zoology, Histology

**Keywords** Platyhelminthes, Land planarians, Alien invasive species, France, Mayotte, Italy, Barcoding, Citizen science, Mitogenome, Taxonomy

## INTRODUCTION

Many new records of alien land planarians (Geoplanidae) have been published in recent years; some correspond to already known species found in new locations, but some are in fact undescribed species, never mentioned in other countries and for which the location of origin is unknown. Recent typical examples include *Obama nungara* Carbayo et al., 2016, a species from South America now invasive in Europe, for which taxonomic confusion has obscured the debate over the last decade ([Carbayo et al., 2016](#); [Justine, Thévenot & Winsor, 2014](#); [Lago-Barcia et al., 2015](#)) and *Caenoplana decolorata* Mateos et al., 2020, probably from Australia ([Justine et al., 2020b](#); [Mateos et al., 2020](#)). In addition to the scientific need for precision, it is important to ascribe precise binomial names to invasive species for administrative purposes.

Although some land planarians show brilliant colours and patterns, these are generally not sufficient for describing species. A formal description should classically be based on both external morphology and microanatomy including that of the copulatory organs, obtained by histological techniques. Modern descriptions generally add partial sequences of a few genes. However, some invasive species have abandoned sexual reproduction and thus lack most characters usable for taxonomy.

Hammerhead flatworms (subfamily Bipaliinae) are among the most spectacular land flatworms, with one species, *Bipalium nobile* Kawakatsu & Makino, 1982, reaching one metre in length (see [Table 1](#) for authors of taxa and key references). In a taxonomic revision of the Bipaliinae, a collective group, the genus *Diversibipalium* Kawakatsu et al., 2002, was erected to accommodate uncertain bipaliid species that had descriptions based on immature specimens, or mature specimens whose internal anatomy, including that of the copulatory organs, has not yet been investigated ([Kawakatsu et al., 2002](#)). All the species assigned to this collective genus are described only on the basis of external morphology and colour pattern. In 2018, we reported two species and assigned them to *Diversibipalium*, but we did not create binomial names; instead, the species were

**Table 1** Hammerhead flatworms (Geoplanidae, Bipaliinae), authors of taxa and key references for biology and mitogenome.

Taxon and authors	Reference for taxon	Main references for biology	Mitochondrial genome
<i>Bipalium kewense</i> Moseley, 1878	<a href="#">Moseley, 1878</a>	<a href="#">Winsor, 1983</a>	<a href="#">Gastineau et al., 2019</a>
<i>Bipalium vagum</i> Jones & Sterrer, 2005	<a href="#">Jones &amp; Sterrer, 2005</a>	<a href="#">Ducey, McCormick &amp; Davidson, 2007</a>	This paper
<i>Bipalium adventitium</i> Hyman, 1943	<a href="#">Hyman, 1943</a>	<a href="#">Ducey et al., 2005</a>	This paper
<i>Bipalium pennsylvanicum</i> Ogren, 1987	<a href="#">Ogren, 1987</a>	<a href="#">Ogren &amp; Sheldon, 1991</a>	Unknown
<i>Diversibipalium multilineatum</i> (Makino & Shirasawa, 1983) Kubota & Kawakatsu, 2010	<a href="#">Makino &amp; Shirasawa, 1983</a>	<a href="#">Makino &amp; Shirasawa, 1986</a>	This paper
<i>Humbertium covidum</i> n. sp.	This paper	<a href="#">Justine et al., 2018</a> ; This paper	This paper
<i>Diversibipalium mayottensis</i> n. sp.	This paper	<a href="#">Justine et al., 2018</a> ; This paper	This paper

**Note:**

The list includes the main invasive taxa and the species studied here.

designated as *Diversibipalium* “black”, found in a single place in France, and *Diversibipalium* “blue”, found only on the island of Mayotte, off Africa ([Justine et al., 2018](#)).

Histology is a technique that requires specialised skills and experience in interpreting sections. In contrast, the development of next generation sequencing technologies (NGS) has made it easier and cheaper to obtain sequences. It is now possible to sequence the organellar genomes of various organisms with a satisfactory rate of success. For land planarians, the first complete mitogenome was described in 2015 ([Solà et al., 2015](#)) from a specimen of *Obama* sp., since then considered to be *Obama nungara* [Carbayo et al., 2016](#) ([Carbayo et al., 2016](#)). Recently, our group supplemented the databases with complete mitogenomes from several other invasive species, namely *Bipalium kewense* ([Gastineau et al., 2019](#)), *Platydemus manokwari* [de Beauchamp, 1963](#) ([Gastineau et al., 2020](#)), *Parakontikia ventrolineata* ([Dendy, 1892](#)) ([Gastineau & Justine, 2020](#)), and *Amaga expatria* [Jones & Sterrer, 2005](#) ([Justine et al., 2020a](#)).

Complete mitogenomes provide a different type of data for molecular identification and phylogeny when compared with the usual molecular markers such as the short and long subunits of the nuclear ribosomal RNA genes (SSU and LSU, respectively). Indeed, the organisation of the mitogenome itself, like gene order, gene composition and the presence of pseudo-genes, can provide an additional phylogenetic signal. Based on our previous experience, phylogenetic trees inferred from mitochondrial protein-coding gene alignments display strong support at their nodes, congruent with taxonomy, classification and biogeography ([Justine et al., 2020a](#)). Also, the use of next generation sequencing rather than PCR coupled with Sanger to obtain mitochondrial genes limits the risk of amplifying nuclear pseudogene copies of mitochondrial DNA, aka numts, which have proven to be a real problem for phylogeny and molecular taxonomy ([Song et al., 2008](#); [Buhay, 2009](#); [Hlaing et al., 2009](#); [Hazkani-Covo, Zeller & Martin, 2010](#); [Leite, 2012](#); [Andújar et al., 2021](#); [Graham, Gillespie & Krehenwinkel, 2021](#)). However, as only five mitogenomes of Geoplanidae were available before this study, there remains a considerable amount of sequencing and documentation of additional taxa yet to be completed. We describe here for the first time the mitochondrial genomes of three already known

species of Bipaliinae, namely *B. vagum*, *B. adventitium* and *D. multilineatum*, and we provide a map for *B. kewense* which was briefly reported without a map ([Gastineau et al., 2019](#)).

In this paper, for the species previously referred as *Diversibipalium* ‘black’ ([Justine et al., 2018](#)), additional material was obtained and we were able to prepare a formal description that includes morphology, histology and molecular phylogenies based on complete mitochondrial genome and nuclear ribosomal genes, and to finally assign this species, on the basis of its anatomy, to the genus *Humbertium* Ogren & Sluys, 2001.

For the second species, *Diversibipalium* ‘blue’, the low number of samples precluded histological investigation, but enough DNA was obtained for us to perform next generation sequencing and retrieve its full mitochondrial genome and nuclear ribosomal genes. We describe it as a new species of the genus *Diversibipalium*, which by definition does not imply any phylogenetic relationships except its appurtenance to the subfamily Bipaliinae. However, all phylogenies inferred from our molecular results positioned this species as the sister-group to all other Bipaliinae, thus suggesting that the species belongs to a different genus yet to be described.

## MATERIALS AND METHODS

### Collection of specimens

New specimens of *Diversibipalium* “black” were provided in the context of a Citizen Science initiative ([Justine et al., 2014, 2015, 2018, 2020a, 2020c, 2021](#)) by Mrs Geneviève Rolland-Martinez, from her garden in Billère, Department of Pyrénées-Atlantiques, France. One of us (ER) collected numerous specimens in a private home garden located in Casier, Province of Treviso, Italy. In both cases, living specimens were sent by post to PG for photography and JLJ and RG for molecular work. Specimens were deposited in the Muséum National d’Histoire Naturelle in Paris, France (MNHN). A specimen of *B. adventitium* was collected in ethanol in Montréal, Québec, Canada on 27 May 2018 by Thomas Théry and deposited as MNHN JL328 ([Justine et al., 2019](#)). A specimen of *B. vagum* was collected in ethanol in Morne Vert, Martinique, Caribbean, on 19 November 2015 by Mathieu Coulis and deposited as MNHN JL307 ([Justine et al., 2018](#)).

### Histology

The specimens were killed in boiling water and fixed in 95% pure ethanol for molecular studies. Specimens for histology were processed and stained by methods provided by [Winsor & Sluys \(2018\)](#). As the specimens were brittle, they were gradually hydrated through a series of descending ethanol solutions to water and softened in Sandison’s fluid until flexible (weeks). Specimens were then divided into anterior, pre-pharyngeal and posterior pieces, rinsed in water, and dehydrated in an ascending ethanol series to 95% ethanol-5% phenol, transferred to Supercedrol® (G.T. Gurr Ltd, London, UK), and infiltrated and embedded in Paraplast® paraffin wax, melting point 56 °C (McCormick Scientific). Tissue blocks were sectioned at 7 µm using a Leitz 1,212 rotary microtome, mounted on glass slides with Mayer’s albumen adhesive, stained by Cason’s modification

of Mallory's trichrome along with control sections, and mounted in Entellan® New (Merck-Millipore, Burlington, MA, USA).

Calculation of the Cutaneous Muscular Index (CMI) follows that of [Froehlich \(1955\)](#) and calculation of the Parenchymal Muscular Index (PMI) that of [Winsor \(1983\)](#).

### **Cox1 and LSU sequences obtained by Sanger method**

*Cox1* and LSU sequences were obtained by Sanger sequencing as detailed in [Justine et al. \(2018\)](#).

We built a tree and evaluated distances between all partial *cox1* sequences available for the species previously referred to as *Diversibipalium* "black" from three localities. All alignment and analyses were conducted with MEGA7 ([Kumar, Stecher & Tamura, 2016](#)). After choosing the best model, which was the Hasegawa-Kishino-Yano model, an ML tree was constructed ([Hasegawa, Kishino & Yano, 1985](#)). A neighbour-joining (NJ) tree was constructed for comparison. Distances were analysed following routine methods ([Justine et al., 2018](#)).

### **Next generation sequencing and phylogeny**

Samples of tissues conserved in ethanol 70% were sent to the Beijing Genomics Institute (BGI-Shenzhen, Shenzhen, China), which performed DNA extraction, library preparation and sequencing on a DNBSEQ platform. For each sample, a total of ca. 60 million clean 100 bp paired-end reads were obtained and assembled using SPAdes 3.14.0 ([Bankevich et al., 2012](#)) with a k-mer of 85. The contigs corresponding to mitogenomes were verified using Consed ([Gordon, Abajian & Green, 1998](#)). Genes were identified with the help of MITOS ([Bernt et al., 2013](#)), but also required manual curation on several occasions. rRNAs were obtained by alignments with reference sequences from *O. nungara* and *B. kewense*, and tRNAs were found using MITOS. In some cases, tRNAs were also checked with ARWEN command line using the -gcflatworm option ([Laslett & Canbäck, 2008](#)). All genomic maps were drawn using OGDRAW ([Lohse et al., 2013](#)). LOGOs were obtained from WebLogo3 online ([Crooks et al., 2004](#)). When needed, alignments were printed out using GenDoc ([Nicholas, Nicholas & Deerfield, 1997](#)).

SSU and LSU sequences were retrieved from the contig files obtained after assembly, by basic data mining using blastn command line and earlier references obtained by PCR as a database ([Boratyn et al., 2012](#)).

Four separate phylogenies were constructed, based on the partial nuclear ribosomal small subunit gene (SSU), the partial nuclear ribosomal large subunit gene (LSU), the concatenated amino-acid sequences of all mitochondrial proteins, and concatenated *cox1*, SSU and LSU genes. For SSU, 14 different sequences were used, and 20 for LSU with, in both cases the Geoplaninae *O. nungara* and *A. expatria* as outgroups. For the mitochondrial protein phylogeny, sequences obtained from 19 organisms were used, but here the outgroup was *Prosthiosomum siphunculus* Delle Chiaje, 1822 (Polycladida). The three-gene phylogeny (*cox1*, SSU, LSU) was performed on the same species as those included in the mitochondrial protein phylogeny, minus those for which SSU or LSU data were missing, plus the species *Novibipalium venosum* (Kaburaki, 1922) and *Bipalium*

*nobile*, for which *cox1* sequences [HM346599](#) and [MG436936](#) were used, respectively. Otherwise, all *cox1* sequences were derived from whole mitogenomes, and SSU and LSU sequences correspond to those included in their respective trees. In total, 19 organisms were included in the three-gene phylogeny. The single genes and concatenated sequences were aligned using MAFFT 7 ([Katoh & Standley, 2013](#)) with the -auto function. For both concatenated datasets, the resulting alignments were trimmed by trimAl ([Capella-Gutiérrez, Silla-Martínez & Gabaldón, 2009](#)) with the -automated1 function. The final sizes of the trimmed alignments were 2,587 AA for the mitochondrial protein dataset and 3,447 bp for the three-gene dataset. For the SSU, LSU and three-gene phylogenies, the evolution model was GTR+I+G, chosen according to jModelTest2 ([Darriba et al., 2012](#)), while for the mitochondrial protein phylogeny it was mtART+I+G, chosen *ad hoc* as a model for mitochondrial protein coding genes of invertebrates ([Abascal, Posada & Zardoya, 2007](#)). Maximum likelihood (ML) phylogenies were all conducted using RaxML 8.0 ([Stamatakis, 2014](#)), with the best tree out of 100 being computed for 1,000 bootstrap replicates. Bayesian inference (BI) phylogenies were conducted on MrBayes 3.2.7 ([Ronquist et al., 2012](#)) using the default parameters, on alignments transformed into the nexus format by ALTER ([Glez-Peña et al., 2010](#)). Due to the absence of the mtART model in MrBayes 3.2.7, no BI phylogeny was performed on the concatenated mitochondrial protein sequences. The average standard deviations of split frequencies attained by MrBayes at the end of the run were 0.005317, 0.003415 and 0.001453 for the SSU, LSU and three-gene phylogenies, respectively.

### Detection of alien DNA

For all the samples sequenced in this study, data mining was performed on the contigs obtained after assembly to find potential traces of alien DNA, using blastn command line ([Boratyn et al., 2012](#)) and a database consisting of SSU sequences from *Eisenia fetida* Savigny, 1826 ([EF534709](#)), *Helix aspersa* Müller, 1774 ([MK919694](#)) and *Schistocerca pallens* Thunberg, 1815 ([KM853186](#)).

### Compliance with the international commission on zoological nomenclature

The electronic version of this article in Portable Document Format (PDF) will represent a published work according to the International Commission on Zoological Nomenclature (ICZN), and hence the new names contained in the electronic version are effectively published under that Code from the electronic edition alone. This published work and the nomenclatural acts it contains have been registered in ZooBank, the online registration system for the ICZN. The ZooBank LSIDs (Life Science Identifiers) can be resolved and the associated information viewed through any standard web browser by appending the LSID to the prefix <http://zoobank.org/>. The LSID for this publication is: urn:lsid:zoobank.org:pub:27A4D685-9042-40C2-A40A-89FF8BCC489B. The online version of this work is archived and available from the following digital repositories: PeerJ, PubMed Central SCIE and CLOCKSS.

## RESULTS

### Description of *Humbertium covidum*

#### Taxonomy

Order Tricladida Lang, 1884 ([Lang, 1884](#))

Suborder Continenticola Carranza, Littlewood, Clough, Ruiz-Trillo, Baguña & Riutort, 1998 ([Carranza et al., 1998](#))

Family Geoplanidae Stimpson, 1857 ([Stimpson, 1857](#))

Subfamily Bipaliinae von Graff, 1896 ([von Graff, 1896](#))

Genus *Humbertium* Ogren & Sluys, 2001 ([Ogren & Sluys, 2001](#))

#### *Humbertium covidum* n. sp.

urn:lsid:zoobank.org:act:3847E9FE-463B-4FDB-A164-88765A52D65A

Synonym: *Diversibipalium* “black” of [Justine et al. \(2018\)](#)

Type-locality: Garden in Casier, county of Casier, Province of Treviso, Region of Veneto, Italy. Coordinates: E 12.289391, N 45.639459. Collected by Enrico Ruzzier on 30th September 2019.

Type-material: Holotype MNHN JL351B (36 microslides anterior LSS, pre-pharyngeal TS and posterior LSS in a single block) and Paratypes MNHN JL351A (34 microslides TS anterior half and LSS posterior portion in a single block); 14 Paratypes (MNHN JL351C-G and JL351Q-Y) retained whole.

Additional material and localities: MNHN JL090, six specimens, domestic garden in Saint-Pée-sur-Nivelle, Department of Pyrénées Atlantiques, France, collected 12 November 2013; MNHN JL343, one specimen, domestic garden in Billère, Department of Pyrénées Atlantiques, France, collected 14 May 2019.

Behaviour and habitat: In Casier, Italy, the species was the only flatworm found; numerous specimens were swarming, and the species was active in the earliest hours of the morning, not during late evening or at night. The two records from France were from gardens where *Bipalium kewense* was also found.

Molecular information: MNHN JL090 from Saint-Pée-sur-Nivelle: partial *cox1* sequence from Sanger sequencing [MG655588](#) ([Justine et al., 2018](#)); partial LSU from NGS, [MZ520989](#) (this paper); partial SSU from NGS, [MZ520996](#) (this paper); complete mitogenome [MZ561471](#) (this paper). MNHN JL343 from Billère: partial *cox1* sequence from Sanger sequencing, [MZ622153](#) (this paper). MNHN JL 351 from Casier, partial *cox1* sequence, five replicates from Sanger sequencing [MZ622148–MZ622152](#) (this paper); partial LSU, three replicates from Sanger sequencing [MZ647546–MZ647548](#) (this paper); partial LSU from NGS [MZ520988](#) (this paper); partial SSU from NGS [MZ520995](#) (this paper); complete mitogenome [MZ561472](#) (this paper). See [File S1](#) for details.

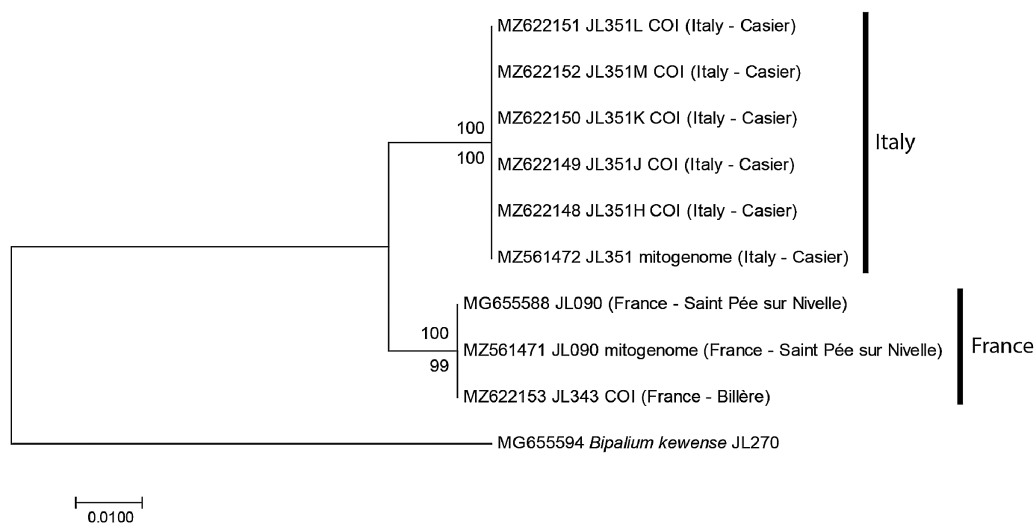


**Figure 1** *Humbertium covidum* n. sp. from two populations, tree based on *cox1* sequences. The evolutionary history was inferred using the Maximum Likelihood and the Neighbour-Joining methods; there was a total of 387 positions in the final dataset. All partial *cox1* sequences from Italy (six specimens) were identical, as were the three sequences from France, from two localities. Sequences from France and Italy differed by 2.58%. Bootstrap values: above branches, ML; below branches, NJ.

Full-size DOI: [10.7717/peerj.12725/fig-1](https://doi.org/10.7717/peerj.12725/fig-1)

Etymology: The specific name *covidum* was chosen as homage to the numerous casualties worldwide of the COVID-19 pandemic. Furthermore, a large part of this study was written during the lockdowns.

### Similarity of *cox1* sequences from various populations

For the specimens from Casier, Italy, we had six *cox1* sequences, including five from Sanger sequencing (MNHN JL351H, J, K, L, M) and one from the NGS mitogenome. In addition, we had the *cox1* sequence of one specimen from Billère, Pyrénées Atlantiques (MNHN JL343) and the *cox1* sequences of two specimens MNHN JL090 from Saint-Pée-sur-Nivelle, Pyrénées Atlantiques, mentioned in our 2018 paper (Justine et al., 2018) and described as *Diversibipalium* sp. “black”, one from Sanger sequencing and one from the NGS mitogenome. The ML and NJ trees (Fig. 1) built from these nine sequences, and one sequence of *B. kewense* as the outgroup were identical and showed that sequences were separated into two clades: one clade included all sequences from France (both from Billère and Saint-Pée-sur-Nivelle) and all these sequences were identical; one clade included all sequences from Italy and all these sequences were identical. The differences between two clades involved 10 positions out of 387, i.e., the distance based on partial *cox1* sequences was 2.58%.

### Diagnosis

Specimens of *Humbertium* with reniform-shaped headplate, with dark brown to black dorsal ground colour, without stripes or other ornamentation, ventral surface light grey–greyish brown with paler creeping sole; eyes in a triple row around anterior headplate, present dorso-laterally on headplate, ventrally behind the lappets, continuing



along the sides of the body in a staggered row posteriorly; pharynx plicate; testes ventral, extending from behind ovaries to pharynx; vas deferens enter penis bulb separately; penis bulb small, strongly muscularised; penis almost horizontal, elongate, tapered; male atrium almost horizontal then steeply inclined ventrally; female genital canal almost vertical, in two parts with shell glands opening into the proximal canal; ovovitelline ducts ascend dorsally before the gonopore to enter the proximal female glandular canal antero-dorsally; the male and female efferent ducts are contained within a muscular genital pad through which the female canal opens to the left and slightly dorsal to the male canal, both entering the common genital canal slightly posterior and above the gonopore. A viscid gland is present in the genital pad anterior to the male efferent duct. The efferent canals open into a narrow horizontal highly glandular common genital canal. The common canal opens into the common atrium, in which the gonopore is centrally placed ventrally.

### **Morphology**


Photographs of specimens are presented for live specimens from Italy (Figs. 2–5) and Billère in France (Figs. 6–10) and preserved specimens from Saint-Pée-sur-Nivelle (Figs. 11, 12). Headplate reniform with rounded non-recurved lappets, with width of headplate in living specimens about 1.3 times the maximum body width, and headplate length to width ratio 1:1.6–2.7 (measured from scaled drawings of photographs of living specimens, Fig 19 *Justine et al., 2018*), and 0.8 times the maximum body width in preserved specimens. Living specimens attain a length of 20–25 mm, and preserved specimens 9–20 mm in length, with the body width:length ratio 1:4.5–1:5.7. Dorsal ground colour dark brown to black, with no evidence of dorsal stripes or bands on body or headplate (Figs. 2, 3, 5, 6). Ventral surface light grey to greyish-brown colour with pale grey creeping sole (Figs. 3, 4). Dimensions of preserved sexual specimens are provided in Table 2 and Figs. 11, 12.

### **Internal anatomy**


#### Body wall and musculature

These characteristics are shown in Figs. 13, 14. The epithelium is thicker dorsally (28–32  $\mu\text{m}$ ) than ventrally (12–21  $\mu\text{m}$ ). Three types of rhabdoids are present: large xanthophil chondrocytes measuring 23.8  $\times$  5.6  $\mu\text{m}$  to 30.8  $\times$  4.2  $\mu\text{m}$  (length  $\times$  width) predominate over the dorsum to the marginal zone, and xanthophil rhammites measuring 21.0  $\times$  1.4  $\mu\text{m}$ –25.2  $\times$  2.8  $\mu\text{m}$  (length  $\times$  width) also cover the same area but are less numerous. Both the chondrocytes and rhammites project slightly above the epithelium. Micro-rhabdites (*stäbschen*) 2.8–4.2  $\mu\text{m}$   $\times$  0.7  $\mu\text{m}$  (length  $\times$  width) are present in the ventral epithelium, mainly either side of the creeping sole. Of the epidermal secretions, xanthophil secretions predominate over the dorsum to the marginal zone, with erythrophil and cyanophil granular secretions relatively sparse except over the creeping sole, with a small concentration of erythrophil secretions either side of the slight central protuberance on the creeping sole. Epidermal secretions on the headplate reflected those of the rest




**Figure 2** *Humbertium covidum* n. sp. from Italy, alive. General dorsal aspect. Photo by Pierre Gros.  
Full-size  DOI: 10.7717/peerj.12725/fig-2




**Figure 3** *Humbertium covidum* n. sp. from Italy, alive. Lateral view showing locomotion and slime trail. Photo by Pierre Gros.  
Full-size  DOI: 10.7717/peerj.12725/fig-3



**Figure 4** *Humbertium covidum* n. sp. from Italy, alive. Individual with raised anterior end showing ventral surface. Photo by Pierre Gros.  
Full-size  DOI: 10.7717/peerj.12725/fig-4



**Figure 5** *Humbertium covidum* n. sp. from Italy, alive. Ventral surface with typical headplate shape. Photo by Pierre Gros. [Full-size](#)  DOI: 10.7717/peerj.12725/fig-5



**Figure 6** *Humbertium covidum* n. sp. from Billère, France, alive. General dorsal aspect. Photo by Pierre Gros. [Full-size](#)  DOI: 10.7717/peerj.12725/fig-6



**Figure 7** *Humbertium covidum* n. sp. from Billère, France, alive. Lateral aspect. Photo by Pierre Gros. [Full-size](#)  DOI: 10.7717/peerj.12725/fig-7



**Figure 8** *Humbertium covidum* n. sp. from Billère, France, alive. Lateral aspect showing extended papillae on headplate. Photo by Pierre Gros. [Full-size !\[\]\(5f471a71b78d7676bc356df190b88ab4\_img.jpg\) DOI: 10.7717/peerj.12725/fig-8](https://doi.org/10.7717/peerj.12725/fig-8)



**Figure 9** *Humbertium covidum* n. sp. from Billère, France, alive. Individual with raised anterior end. Photo by Pierre Gros. [Full-size !\[\]\(e6d8ed0e56026ff17854aa495380637d\_img.jpg\) DOI: 10.7717/peerj.12725/fig-9](https://doi.org/10.7717/peerj.12725/fig-9)

of the body. All epidermal secretions are derived from mesenchymal secretory cells. There is no evidence of a glandular margin. Fine black granular pigment is sparsely scattered throughout the dorsal mesenchyme, though it was noted that Sanderson's fluid



**Figure 10** *Humbertium covidum* n. sp. from Billère, France, alive. The flatworm seems to threaten a snail (unidentified species). Photo by Pierre Gros. [Full-size !\[\]\(b345a1c4255362eec3746050dd71ccac\_img.jpg\) DOI: 10.7717/peerj.12725/fig-10](https://doi.org/10.7717/peerj.12725/fig-10)



**Figure 11** *Humbertium covidum* n. sp. from Saint-Pée-sur-Nivelle, France, preserved. Specimen MNHN JL090, preserved specimen, dorsal aspect. Showing the partly protruded pharynx. Photo by Jean-Lou Justine. Reproduced from Figure 20 of *Justine et al. (2018)*.

[Full-size !\[\]\(74d4806277d7e73349d8e8c0897931e9\_img.jpg\) DOI: 10.7717/peerj.12725/fig-11](https://doi.org/10.7717/peerj.12725/fig-11)

appeared to elute some black dorsal pigment. The ciliated creeping sole is 21.6–30.8% of the body width and is slightly protuberant centrally and bears an insunk ciliated epithelium.



**Figure 12** *Humbertium covidum* n. sp. from Saint-Pée-sur-Nivelle, France, preserved. Specimen MNHN JL090. Preserved specimen, ventral aspect. The ventral ground colour is grey, with the creeping sole a lighter tone. The pharynx is slightly protruded from the mouth, and the gonopore is evident as a small transverse white slit on the creeping sole some 2 mm below to the mouth. Scale is in mm. Photo by Jean-Lou Justine. Reproduced from Figure 21 of *Justine et al. (2018)*.

Full-size  DOI: [10.7717/peerj.12725/fig-12](https://doi.org/10.7717/peerj.12725/fig-12)

Cutaneous musculature is tripartite and very weakly developed, comprising circular muscle represented by a single fibre, single decussate diagonal fibres, and longitudinal muscles in small bundles of 2–3 fibres each, CMI 2–3%.

Parenchymal musculature consists of a strong ventral plate of longitudinal muscles extending laterally to the mid-lateral region and divided into uneven bundles of 4–10 fibres by dorsoventral muscles, with weak supraneural and dorsal parenchymal longitudinal muscles present as single fibres. Strong dorsal transverse muscles and weak suprainestinal and dorsoventral muscles are present. PMI 8.4–15% of which the dorsal transverse muscles contribute the greater amount.

#### Alimentary system

The pharynx is collar-form (*Fig. 15*), with the dorsal insertion in the posterior third of the pharyngeal pouch and posterior to the mouth, and the ventral insertion anterior to the mouth. The outer pharyngeal musculature comprises an ectal single fibre of longitudinal muscle underlain by circular muscles and an ental layer of longitudinal muscles. The inner musculature consists of a single longitudinal muscle fibre underlying the insunk epithelium, underlain by sheaths of circular and longitudinal muscles (derived

**Table 2** *Humbertium covidum* n. sp.: dimensions of specimens examined.

Fixed specimen dimensions	Holotype JL 351A	Paratype JL 351A	Paratype JL 351A	Paratype JL 351A	Paratype JL 351A	Voucher JL 090
Geographic origin	Italy	Italy	Italy	Italy	Italy	France
Length (mm)	13.3	12.0	13.2	12.8	9.0	20.0
Width of headplate (mm)	2.0	NM	2.0	2.0	2.0	NM
Width at mouth (mm)	2.5	2.1	2.5	2.5	2.4	3.2
Ratio width headplate to body width	0.8:1	–	0.8:1	0.8:1	0.8:1	–
Ratio body width to length	1:5.3	1:5.7	1:5.3	1:5.1	1:4.5	1:6.3
Mouth (mm)	5.0 (37.6)	5.6 (46.7)	6.5 (49.2)	6.0 (46.9)	6.0 (66.7)	6.0 (30.0)
Gonopore (mm)	7.1 (53.4)	7.5 (62.5)	8.2 (62.1)	7.8 (60.9)	7.4 (82.2)	7.8 (39.0)
Distance mouth-gonopore (mm)	2.1 (15.8)	1.9 (19)	1.7 (12.9)	1.8 (14.1)	1.4 (15.6)	1.8 (9)
Body Height $\mu\text{m}$	1,157	741				
Creeping sole width $\mu\text{m}$ (% body width)	1,157 (30.8%)	647 (21.6%)				
CMI	2%	3.2%				
PMI	8.4%	15%				
Pharynx type	Collar	Bell-Collar				
Pharyngeal pouch length (% body length)	1 068 $\mu\text{m}$ (8%)	1 287 $\mu\text{m}$ (10%)				
Position of mouth in pharyngeal pouch	623 $\mu\text{m}$ (58.5%)	624 $\mu\text{m}$ (48.5%)				
Distance between posteriad pharyngeal pouch and antieriad penis bulb	250 $\mu\text{m}$	590 $\mu\text{m}$				

**Note:**

Positions of body apertures are measured from the anterior tip. Figures in parentheses are the position of the aperture expressed as a percentage of body length. NM: not measured.

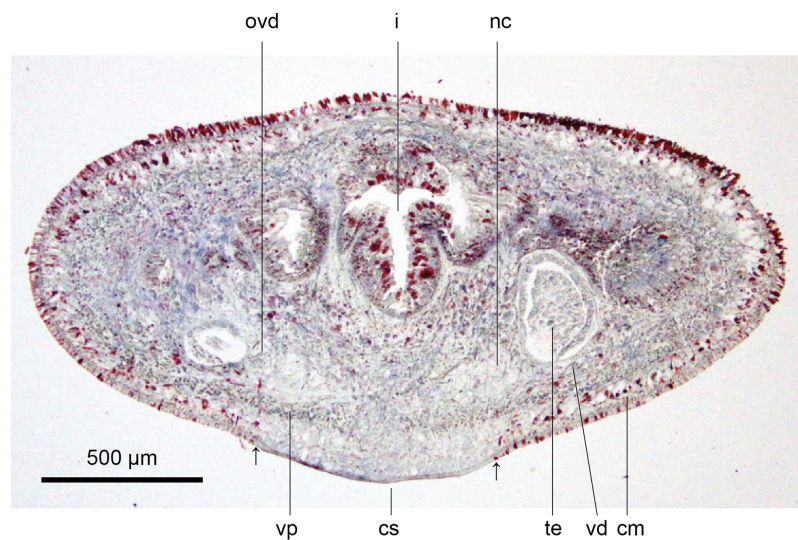


**Figure 13** Anatomy of *Humbertium covidum* n. sp., pre-pharyngeal region. Holotype, specimen MNHN JL351B. Pre-pharyngeal region, transverse section. Arrows indicate the extent of the creeping sole. Photo by Leigh Winsor.

Full-size  DOI: [10.7717/peerj.12725/fig-13](https://doi.org/10.7717/peerj.12725/fig-13)

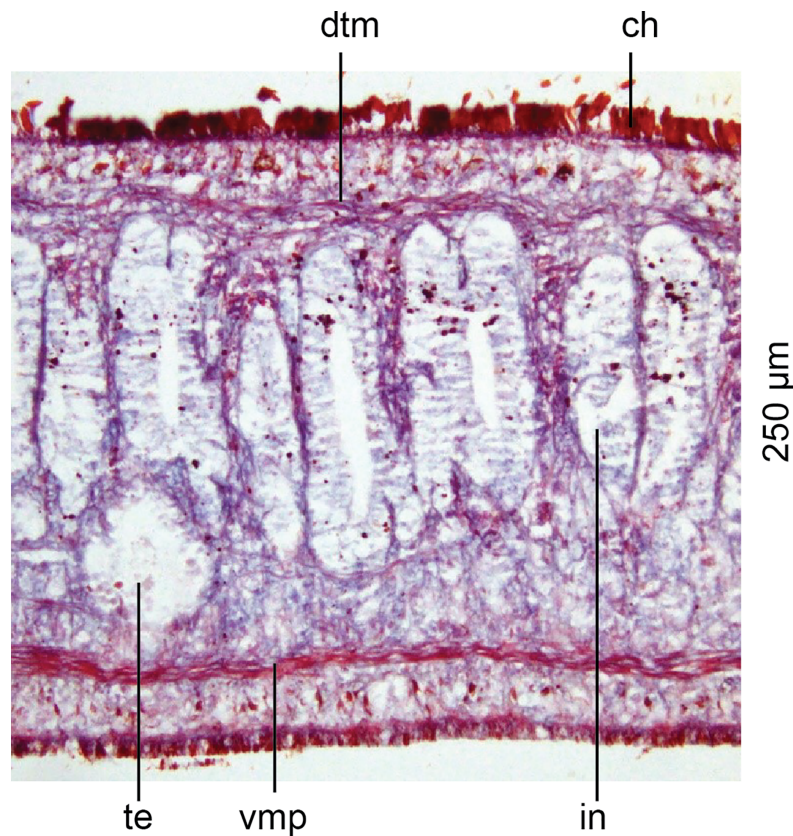


**Figure 14** Anatomy of *Humbertium covidum* n. sp, ventral longitudinal muscular plate. Holotype, specimen MNHN JL351B. Lateral body showing ventral longitudinal muscular plate. Photo by Leigh Winsor. [Full-size !\[\]\(5fd6ef84f97f42d7f8b34275f1b65312\_img.jpg\) DOI: 10.7717/peerj.12725/fig-14](https://doi.org/10.7717/peerj.12725/fig-14)

planariid type). Radial muscles, erythrophil, xanthophil and cyanophil secretory ducts make up the mid-pharyngeal wall. The pharyngeal pouch is 1,068–1,342  $\mu\text{m}$  long, representing 8–10% of the total body length. The mouth is situated in the approximate mid-ventral region of the pouch. Oesophagus absent.

#### Sensory organs

The sensorial zone contours the anterolateral sub-margin of the headplate and consists of flat tooth-like aciliate papillae about 55  $\mu\text{m}$  high and 38  $\mu\text{m}$  wide separated from each other by a groove of 10  $\mu\text{m}$ , with about 20 papillae per millimetre. Ciliated pits about 20  $\mu\text{m}$  deep and 4  $\mu\text{m}$  wide open just below the lips of the papillae.

Eyes are present as a triple row contouring the anterior margin of the headplate, with extension dorso-laterally, and ventrally behind the lappets, then continuing posteriorly along the body sides in a staggered row (Fig. 16). The eyes are pigment cup ocelli of similar shape and size, about 16  $\mu\text{m}$  in diameter, with two retinal clubs per ocellus.

#### Reproductive organs

The ovaries are spheroidal, 150  $\mu\text{m}$  in diameter, located almost a millimetre behind the anterior margin of the headplate and are half embedded in the ventral nerve cords.



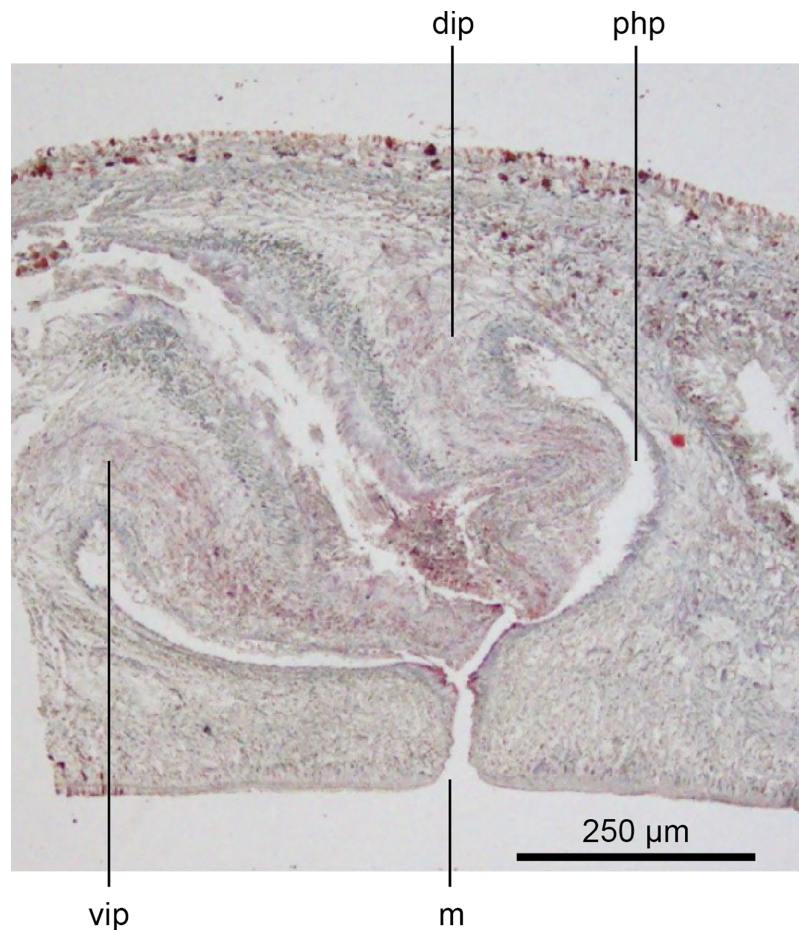


**Figure 15** Anatomy of *Humbertium covidum* n. sp., pharynx. Holotype, specimen MNHN JL351B. Pharynx, sagittal section. Photo by Leigh Winsor. [Full-size !\[\]\(fcc3264021d438d9732560e78099f674\_img.jpg\) DOI: 10.7717/peerj.12725/fig-15](https://doi.org/10.7717/peerj.12725/fig-15)

The testes are ventral, round to ovoid in shape about 300  $\mu\text{m}$  high and 220  $\mu\text{m}$  in diameter and extend uniserially from behind the ovaries posteriorly to the pharynx. They open towards the lower testicular pole *via* short sperm ductules into the vasa deferentia. The vasa deferentia of both sectioned specimens of *Humbertium covidum* contained mature spermatozoa. In both specimens, the testes are at different stages of maturity with those nearest the copulatory organs containing mature spermatozoa.

The copulatory organs (Figs. 17, 18) lie 250–590  $\mu\text{m}$  behind the pharyngeal pouch. The male organ rises 20° dorsad from the horizontal and the male atrium dips steeply 50° ventrad, with the female organ almost vertically positioned (10° from the vertical towards the posterior).

#### Male organs

The protrusible penis comprises a small but highly muscular bulb, with an elongate, ventrally curved, and tapered finger-like papilla opening towards the left-hand side, and filling most of the conical male atrium. The lumen of the seminal (prostatic) vesicle is 50–60  $\mu\text{m}$  in diameter and lined by a cuboidal secretory epithelium receiving fine granular

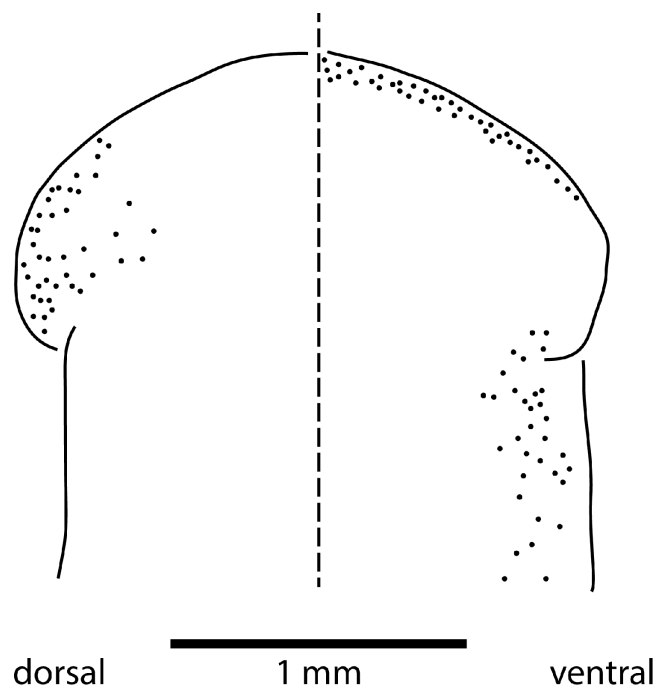


**Figure 16** Morphology of *Humbertium covidum* n. sp., eye pattern. Paratype JL 351C. Headplate showing the dorsal and ventral eye patterns in a cleared specimen. The headplate is curled ventrad. Drawing by Leigh Winsor. [Full-size !\[\]\(1663bb69f307a960345edb0e712f8c02\_img.jpg\) DOI: 10.7717/peerj.12725/fig-16](https://doi.org/10.7717/peerj.12725/fig-16)

erythrophil secretions from erythrophil mesenchymal glands surrounding the bulb. This epithelium grades into a tall voluminous nucleate columnar epithelium penetrated by the expanded terminal ducts of mesenchymal erythrophil glands external to the bulb, discharging secretions into the proximal ejaculatory duct. At about the point where the penis bends towards the gonopore, the lining of the ejaculatory duct transitions to a cuboidal epithelium of the distal ejaculatory duct with a reduction in secretions and height, and from there grades to the flat nucleate-facing epithelium of the distal penis papilla.

The dorsal half of male atrium is lined by a low-facing epithelium and the ventral half lined by a low nucleate columnar epithelium that also covers the proximal external penis. Distally the atrium is lined by a low-facing epithelium. An inner strong sheath of circular muscles and an external sheath of longitudinal muscles underlie the atrial epithelium.

Musculature of the penis bulb consists of a strong outer sheath of broad bands of longitudinal muscles between which oblique muscles are interwoven. The ejaculatory duct is surrounded by a strong inner layer of circular muscles underlain by mixed longitudinal and circular muscles, with a sheath of circular muscles underlying the outer penial epithelium.

The vasa deferentia, lined by a cuboidal epithelium, lie lateral to and on the same level as the ovovitelline ducts, and just below the testes with which they communicate *via* a short sperm ductule. Passing posteriorly, they continue to the level of the penis bulb where

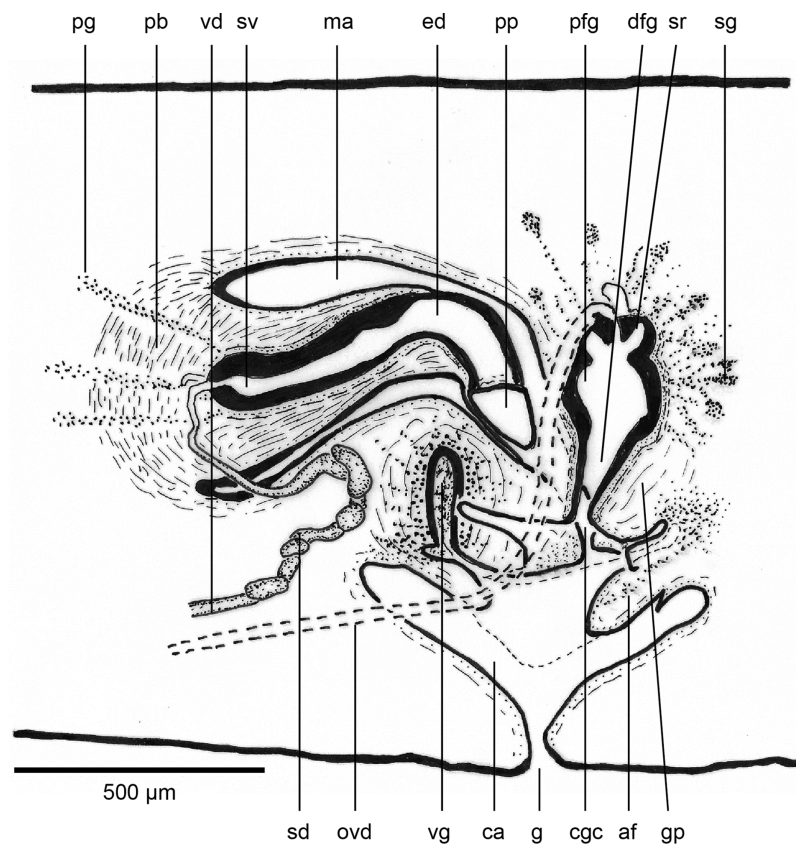


**Figure 17** Anatomy of *Humbertium covidum* n. sp., composite drawing of copulatory organs. Holotype, specimen MNHN JL351B. Composite reconstruction of the copulatory organs, sagittal view. The dashed line in the common atrium indicates the extent of the glandular mesenchyme forming the common genital canal. Anterior: left. Drawing by Leigh Winsor.

Full-size  DOI: [10.7717/peerj.12725/fig-17](https://doi.org/10.7717/peerj.12725/fig-17)

they gently rise, expand to form spermiducal vesicles and recurve, piercing the anterior penis bulb to separately open into the seminal vesicle.

#### Female organs

The glandular canal is aligned almost at right angles to the ventral surface, is about 370  $\mu\text{m}$  in length, and is divided into two distinct parts—the proximal (dorsad) section, and the distal (ventrad) section: the proximal two-thirds of the glandular canal is thistle-shaped with a maximum diameter of around 220  $\mu\text{m}$ , with a distinct constriction before the centrally invaginated flared blind end where the ovovitelline ducts debouche (could be termed the seminal receptacle). The proximal glandular canal is lined by a tall columnar epithelium with basal nuclei. Secretory ducts, from erythrophil (shell-glands) and cyanophil glands in the surrounding mesenchyme, pierce the epithelium to discharge their contents into the lumen. The fine granular secretions from both types of glands condense within the epithelium and are secreted as membrane-bound masses into the glandular canal. The distal third of the glandular canal, lined by a non-secretory ciliated columnar epithelium, narrows to 70  $\mu\text{m}$  then tapers to 16  $\mu\text{m}$  to discharge into the common genital

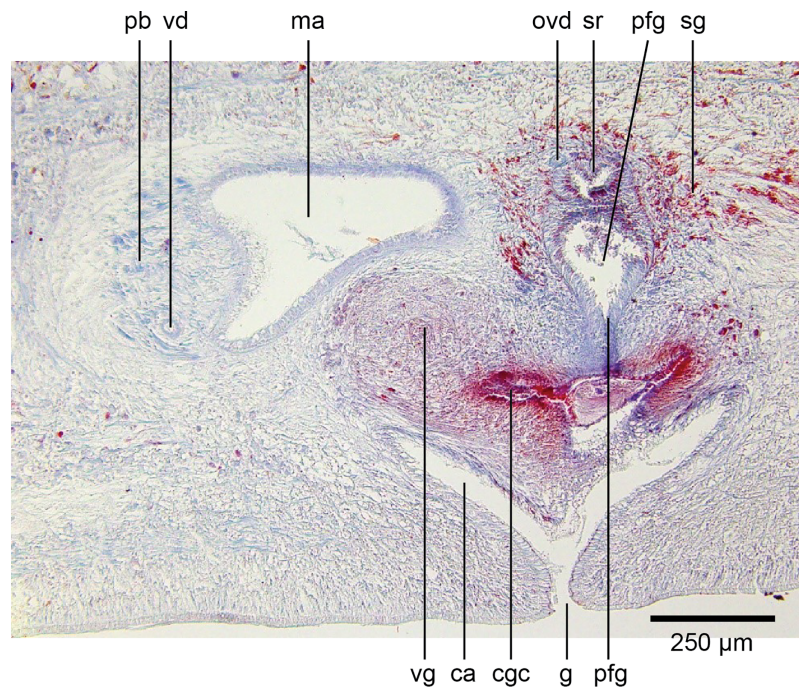


**Figure 18** Anatomy of *Humbertium covidum* n. sp., level of gonopore. Holotype, specimen MNHN JL351B. Copulatory organs at the level of the gonopore, with the female glandular canal entering the common genital canal at the point where it communicates with the common atrium. Anterior: left. Photo by Leigh Winsor. [Full-size !\[\]\(5f471a71b78d7676bc356df190b88ab4\_img.jpg\) DOI: 10.7717/peerj.12725/fig-18](https://doi.org/10.7717/peerj.12725/fig-18)

canal. Underlying the epithelium of the glandular canal is a layer of circular muscles external to which are longitudinal muscles, the whole being invested in a weak muscularis.

The ovovitelline ducts, lined by a ciliated cuboidal epithelium with a circular muscularis, emerge from the lower poles of the ovaries, ascend slightly to pass posteriorly along the lateral margins of the nerve cords. The ovovitelline ducts turn dorsally before the gonopore (holotype JL351B; in the paratype JL351A they turn dorsally about level with the posterior lip of the gonopore some 100  $\mu\text{m}$  posteriad to that figured for the holotype), rise and enter the female glandular canal antero-dorsally, exhibiting the proflexed condition.

#### Common genital canal and common atrium

In the mesenchyme below the male and female organs in the left body wall lies a crescentic band of densely aggregated erythrophil and basiphil glands (Fig. 19). Moving from the left to the right through the mesenchyme, a crescentic split develops in the body wall ventral to the glandular mesenchyme that eventually enlarges to become the common atrium (Fig. 20). At about the same point, an elongate fissure develops horizontally along the mid-band of the glandular mesenchyme, in what becomes the common genital canal on the dorsal side of the fissure. For about 60  $\mu\text{m}$  across the body, the wall of the mesenchyme separates the common genital canal from the common atrium (Fig. 21). The common genital canal is lined by a highly glandular insunk epithelium, richly endowed with granular lightly erythrophil secretions that are secreted as packets of

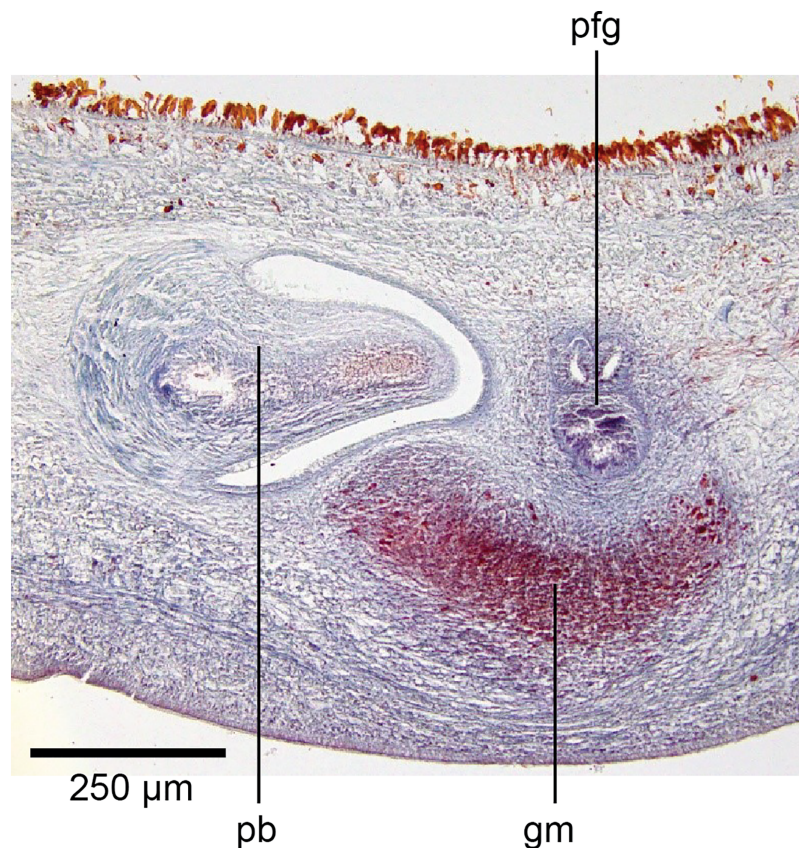


**Figure 19** Anatomy of *Humbertium covidum* n. sp., putative common genital canal. Paratype, specimen MNHN JL351C. Glandular mesenchyme of the putative common genital canal on the left side of the body. Anterior: left. Photo by Leigh Winsor. [Full-size !\[\]\(b345a1c4255362eec3746050dd71ccac\_img.jpg\) DOI: 10.7717/peerj.12725/fig-19](https://doi.org/10.7717/peerj.12725/fig-19)

erythrophil granules, alternating with cyanophil strand secretions, typical of the secretory elements related to cocoon formation. The common atrium is lined by an insunk columnar epithelium, through which amorphous cyanophil secretions are discharged. Commensurate with the appearance of the gonopore, the mesenchymal wall thins to form a residual flap around what becomes a single common atrium. Numerous erythrophil glands discharge their granular secretions into the crease formed between the residual flap and genital pad.

#### Genital pad and viscid gland

The genital pad comprises strong interwoven circular and oblique muscles covered by the same epithelium as the common genital canal. In the anterior pad is situated an ovoid-shaped viscid gland (Figs.22, 23), 280  $\mu$ m high and 120–200  $\mu$ m in diameter, with a duct 160–200  $\mu$ m long and 20–70  $\mu$ m in diameter that opens into the common genital canal. The epithelium of the viscid gland is predominantly charged with finely granular cyanophil secretions, alternating with packets of amorphous dark erythrophil secretions both derived from glands in the surrounding mesenchyme. The secretions discharged into the lumen combine to form thin dark basiphil strands.

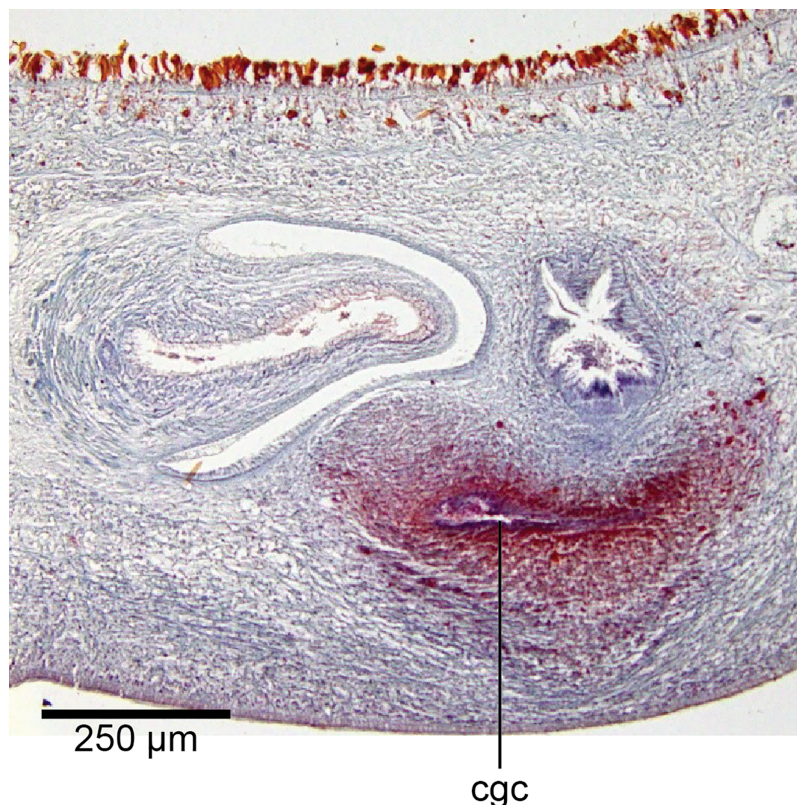


**Figure 20** Anatomy of *Humbertium covidum* n. sp., common genital canal. Paratype, specimen MNHN JL351C. The beginning of the slit-like common genital canal. Anterior: left. Photo by Leigh Winsor.

Full-size  DOI: [10.7717/peerj.12725/fig-20](https://doi.org/10.7717/peerj.12725/fig-20)

Vitellaria are sparse and lie between diverticula of the gut. A genito-intestinal duct is absent.

### **Additional comments**

#### **Fixation**

Stain uptake by the tissue sections of both specimens was suboptimal, in part due to the fixation in 95% ethanol resulting in pronounced tissue vacuolation, and possibly partly due to the prolonged post-fixation treatment in Sandison's fluid. The control tissue sections included with the slides of *Humbertium covidum* verified that the Mallory stain worked perfectly on formaldehyde-fixed tissue.

#### **Pathology**

The larva of a nematode was present in the creeping sole of the holotype.

### **Video file**

A short video file of a living specimen is available as [File S2](#).

### **Occurrences**

The species was recorded in 2013 from a single garden in Saint-Pée-sur-Nivelle (Department of Pyrénées Atlantiques, France) in which *B. kewense* was also present.

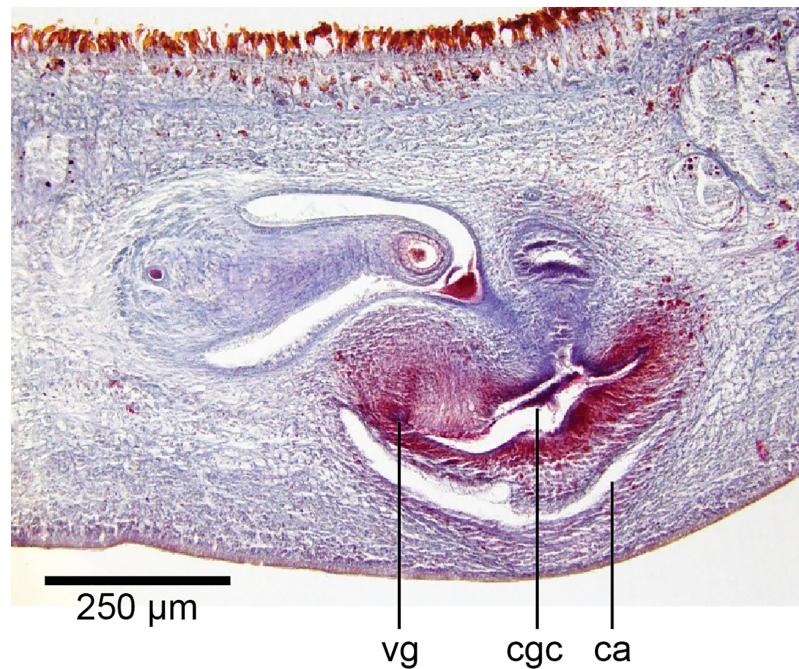


**Figure 21** Anatomy of *Humbertium covidum* n. sp., male atrium. Paratype, specimen MNHN JL351C. The point where the male atrium is about to open into the common genital canal which has not yet opened into the common atrium. Anterior: left. Photo by Leigh Winsor.

Full-size DOI: [10.7717/peerj.12725/fig-21](https://doi.org/10.7717/peerj.12725/fig-21)

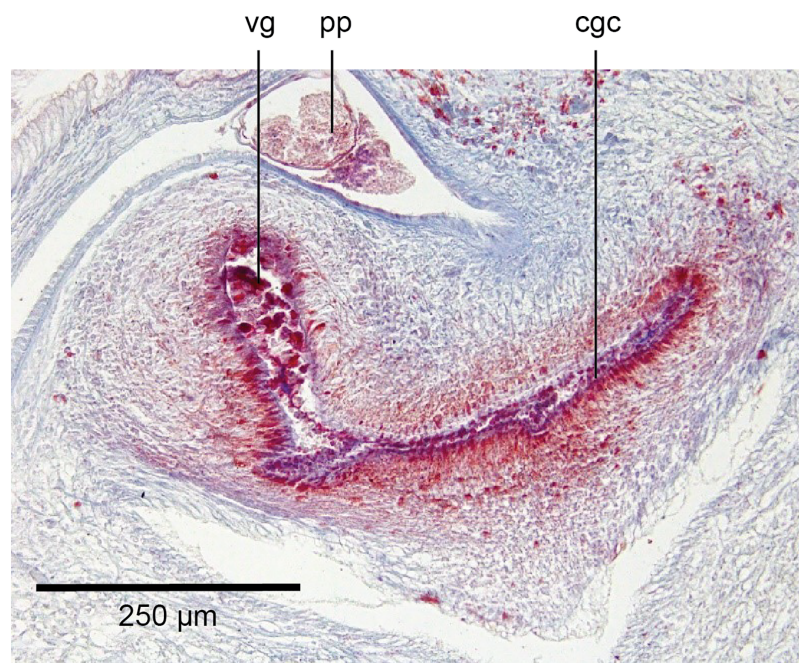


**Figure 22** Anatomy of *Humbertium covidum* n. sp., viscid gland. Holotype, specimen MNHN JL351B. The viscid gland at the anteriad end of the genital pad below the male organs. Anterior: left. Photo by Leigh Winsor.

Full-size DOI: [10.7717/peerj.12725/fig-22](https://doi.org/10.7717/peerj.12725/fig-22)

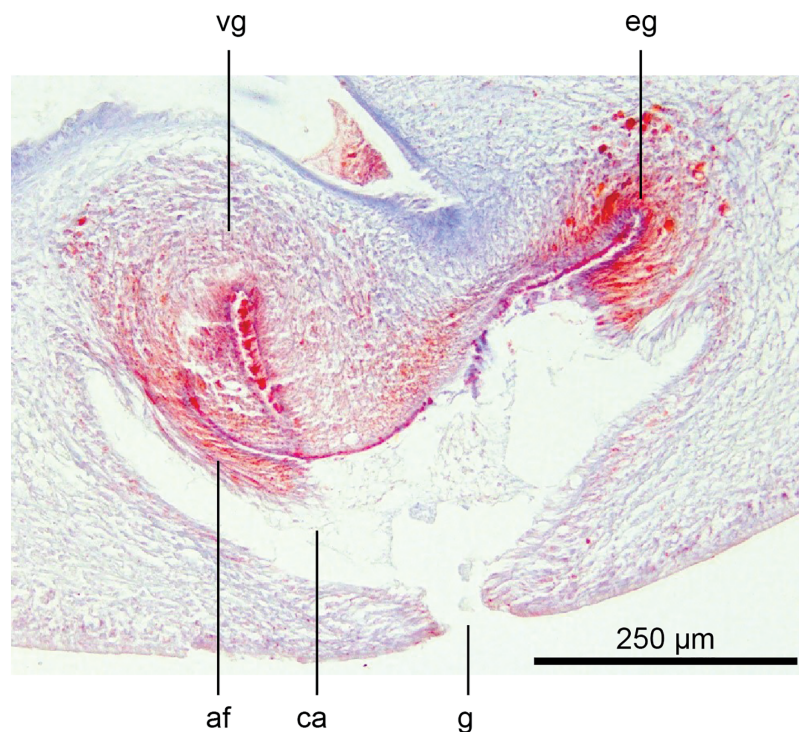


**Figure 23** Anatomy of *Humbertium covidum* n. sp., viscid gland and erythrophil glands. Holotype, specimen MNHN JL351B. The glandular duct of the viscid gland, and erythrophil glands in the atrial crease. Anterior: left. Photo by Leigh Winsor. [Full-size !\[\]\(5fd6ef84f97f42d7f8b34275f1b65312\_img.jpg\) DOI: 10.7717/peerj.12725/fig-23](https://doi.org/10.7717/peerj.12725/fig-23)

According to the owner, the species was present for years in the garden and was still present in 2017. It was then found in a garden in Billère, in the same Department, ca. 100 km from the first location; this garden was also heavily infested with *B. kewense* (Justine et al., 2018). Finally, one of us found in 2019 an abundant population in Casier, Province of Treviso, Italy. In 2019, an intensive campaign on Twitter in various European languages asking for additional reports, did not provide any additional information. In the discussion, we report possible other occurrences in various countries.

### Description of *Diversibipalium mayottensis* n. sp.

#### Taxonomy

Order Tricladida Lang, 1884 (Lang, 1884)

Suborder Continenticola Carranza, Littlewood, Clough, Ruiz-Trillo, Baguña & Riutort, 1998 (Carranza et al., 1998)

Family Geoplanidae Stimpson, 1857 (Stimpson, 1857)

Subfamily Bipaliinae von Graff, 1896 (von Graff, 1896)

Genus *Diversibipalium* Kawakatsu et al., 2002 (Kawakatsu et al., 2002)

#### *Diversibipalium mayottensis* n. sp.

urn:lsid:zoobank.org:act:B59FEE8E-70FD-4DEC-B839-554C351701F8

Synonym: *Diversibipalium* “blue” of Justine et al. (2018).





**Figure 24** *Diversibipalium mayottensis* n. sp, alive. Specimen MNHN JL282 from Mayotte, Indian Ocean, dorsal aspect. The headplate of this small planarian is a rusty-brown colour that extends to some irregular patches on the 'neck.' The dorsal ground colour is an iridescent blue-green ('dark turquoise glitter'). Photo by Laurent Charles. Reproduced from Figure 23 in [Justine et al. \(2018\)](#).


Full-size  DOI: [10.7717/peerj.12725/fig-24](https://doi.org/10.7717/peerj.12725/fig-24)

Type-locality: Ouangani, Mayotte.

Additional localities: Mtsamboro and Mamoudzou, Mayotte.

Type-material: Holotype MNHN JL282, Cascade du Mont Meoni ouaj Coconi, Commune of Ouangani, Mayotte; Coordinates: W 45.12936111, S 12.83522222; Collected on 30 April 2015; Photographed live ([Figs. 24–27](#)); length of preserved specimen 15 mm; *cox1* sequence [MG655598](#). Paratypes: MNHN JL280, Dziani, Commune of Mtsamboro, Mayotte; Coordinates: W 45.08091667, S 12.71208333, 29 April 2015; one specimen, head not visible; length of preserved specimen 7 mm; *cox1* sequence [MG655596](#). MNHN JL281, Dziani, Commune of Mtsamboro, Mayotte; Coordinates: W 45.08758333, S 12.69638889, 29 April 2015; specimen JL281A, length preserved 15 mm, first slightly damaged for Sanger sequencing, later almost completely destroyed for NGS sequencing (only head retained); JL281B, 5 mm; JL281C, length preserved 9 mm; *cox1* sequence [MG655597](#) (based on three identical replicates). MNHN JL283, Convalescence, Commune of Mamoudzou, Mayotte; Coordinates: W 45.18963889, S 12.76891667, 4 May 2015; one specimen, head not visible, preserved 20 mm, alive ca. 30 mm; not sequenced. MNHN JL284, Îlot Mtsamboro, Commune of Mtsamboro, Mayotte; Coordinates: W 45.02769444,



**Figure 25** *Diversibipalium mayottensis* n. sp, alive. Specimen MNHN JL282 from Mayotte, Indian Ocean, dorsal aspect. Same specimen as in Fig. 24. Photo by Laurent Charles. Reproduced from Figure 24 in *Justine et al. (2018)*. Full-size  DOI: [10.7717/peerj.12725/fig-25](https://doi.org/10.7717/peerj.12725/fig-25)

S 12.64247222, 5 May 2015; one specimen, head visible, tail damaged, length preserved 12 mm, *cox1* sequence [MG655599](#). All specimens collected by Laurent Charles. See also [File S1](#).

Behaviour and habitat: In Mayotte, all specimens were collected during the day, under dead wood or leaves, as part of a terrestrial mollusc program. No collection was attempted during the night. All localities were in a slightly degraded natural environment, with little human presence. No research was done to know whether the species was found in gardens, but no citizen science record was received that would suggest this is the case.

Molecular information: All partial *cox1* sequences from 6 specimens listed above were identical; see [Fig. 2](#) in *Justine et al. (2018)*. One specimen (MNHN JL281A) used for NGS sequencing, providing sequences for SSU ([MZ520997](#)), LSU ([MZ520986](#)) and complete mitogenome ([MZ561470](#)).

Etymology: The specific name *mayottensis* refers to the type-locality.

#### **Attribution of the species to *Diversibipalium***

The genus *Diversibipalium* Kawakatsu et al., 2002 is a collective group created to temporarily accommodate species whose anatomy of the copulatory apparatus is still



**Figure 26** *Diversibipalium mayottensis* n. sp, alive regenerating specimen. Dorsal aspect of a regenerating specimen with a damaged anterior end. Specimen MNHN JL280. Under appropriate lighting, the colour of the specimen takes on a beautiful, almost metallic green colour. The iridescence and blue–green colour are lost on fixation, leaving the specimen a dark brown. Photo by Laurent Charles. Reproduced from Figure 25 in *Justine et al. (2018)*. [Full-size !\[\]\(ba1b80118482ccef74a5d718ca4d7242\_img.jpg\) DOI: 10.7717/peerj.12725/fig-26](https://doi.org/10.7717/peerj.12725/fig-26)

unknown (*Kawakatsu et al., 2002*) and it is therefore logical that we attribute the new species to this genus.

### **Diagnosis**

Specimens of *Diversibipalium* with a rusty-brown coloured club-shaped headplate, with iridescent blue green dorsal ground colour in life, dark brown colour when preserved, with the suggestion of a fine white median dorsal stripe; ventral surface light brown with white to pale green coloured creeping sole. The mouth is present in the anterior second fifth of the body, and gonopore in the fourth body fifth.

### **Morphology**

The specimen has the overall morphology of a typical bipaliine, with the headplate of the living specimen is a rusty-brown colour that extends to some irregular patches on the “neck” (Figs. 24, 25). The dorsal ground colour is an iridescent blue green (“dark turquoise glitter”) (Figs. 24–27), with a hint of a fine white median stripe, and the ventral surface a light brown colour, with the creeping sole white to pale green. The iridescence and blue-green colour are lost on fixation, leaving a dark brown ground colour. The posterior margins of the headplate are not recurved but rounded (reniform), giving the headplate a



**Figure 27** *Diversibipalium mayottensis* n. sp, alive regenerating specimen. Dorsal aspect of a regenerating specimen with a damaged anterior end. Specimen MNHN JL280. A small portion of the brown-pigmented ventral surface with the median pale creeping sole can be seen. Photo by Laurent Charles. Reproduced from Figure 26 in *Justine et al. (2018)*.

Full-size  DOI: [10.7717/peerj.12725/fig-27](https://doi.org/10.7717/peerj.12725/fig-27).

club-shape, with width of headplate in living specimens 1.1–1.3 times the maximum body width, and headplate length to width ratio 1:0.6–0.7 (relative dimensions taken from photographs of living specimens in [Figs. 24, 25](#)). The living specimens are up to about 45 mm in length.

A preserved sexual specimen (paratype JL281C), 9 mm long and 1 mm wide, had the mouth situated ventrally approximately 3.5 mm (39% of the body length) from the anterior end, and gonopore 3 mm (33% of the body length) posterior to the mouth. All specimens were used for molecular analysis with the exception of JL 283. In view of the very few specimens available, no specimen was used for histological methods.

## Mitochondrial genomes

### *New mitogenomes for five species*

The main characteristics of all mitogenomes obtained during this study are summarised in [Table 3](#). The genomic maps are also presented for *H. covidum* JL351 ([Fig. 28](#)), *H. covidum* JL090 ([Fig. 29](#)), *D. mayottensis* JL281 ([Fig. 30](#)), *B. vagum* JL307 ([Fig. 31](#)), *B. adventitium* JL328 ([Fig. 32](#)) and *D. multilineatum* JL177 ([Fig. 33](#)). We also present the genomic map of *B. kewense* ([Fig. 34](#)). With the exception of *D. multilineatum* JL177, all

**Table 3** Characteristics of mitogenomes of bipaliines.

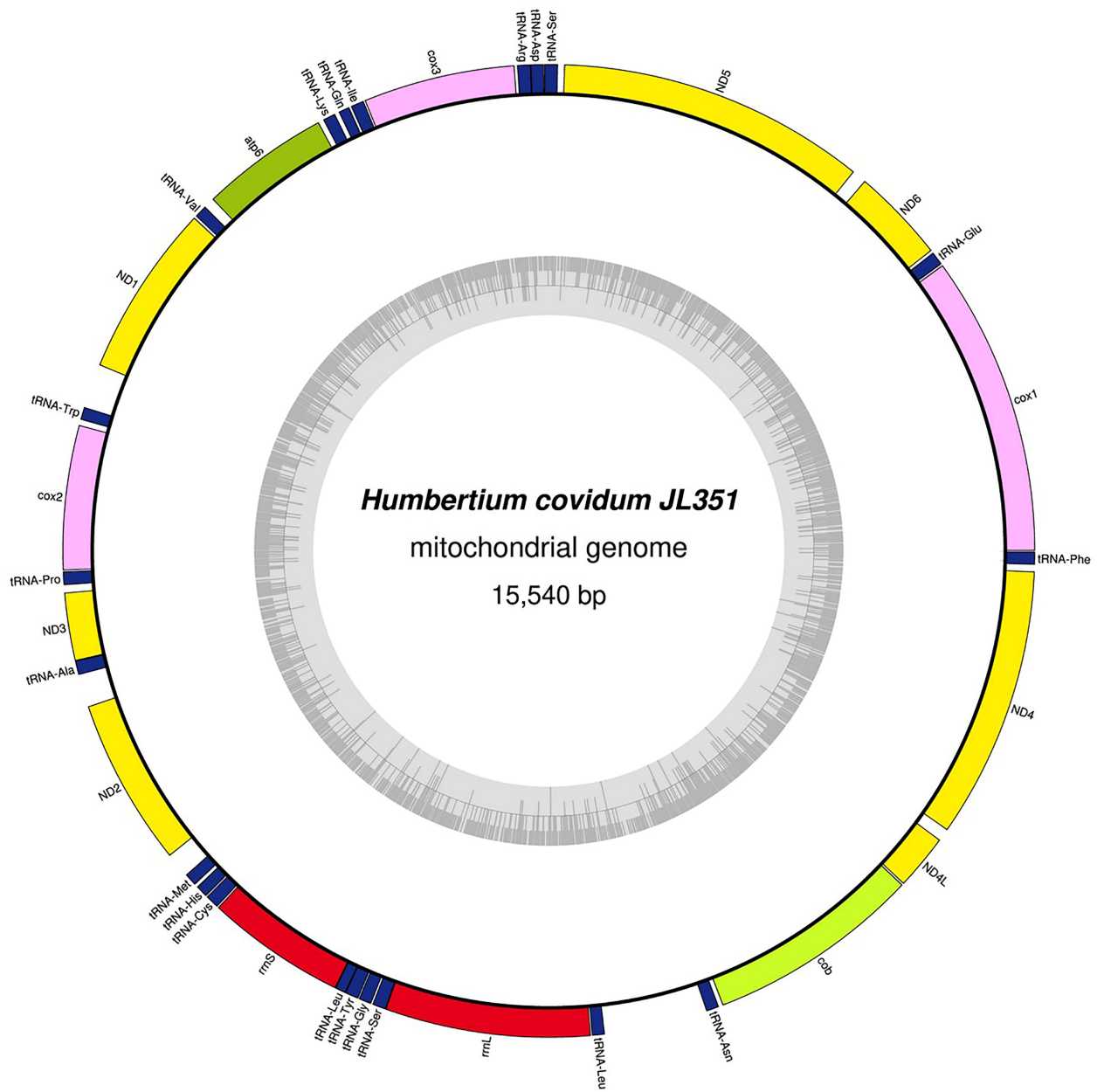
Species	MNHN registration number	GenBank accession number	Size of the mitogenome	Early stop	Alternative start codon
<i>Humbertium covidum</i>	JL351	<a href="#">MZ561472</a>	15,540 bp	<i>ND3</i>	–
<i>Humbertium covidum</i>	JL090	<a href="#">MZ561471</a>	15,524 bp	<i>ND3</i>	–
<i>Diversibipalium mayottensis</i>	JL281	<a href="#">MZ561470</a>	15,989 bp	–	–
<i>Bipalium vagum</i>	JL307	<a href="#">MZ561468</a>	17,149 bp	–	<i>cox3, atp6, ND1, ND4L</i>
<i>Diversibipalium multilineatum</i>	JL177	<a href="#">MZ561469</a>	15,660 bp (not complete)	–	<i>ND2, ND3</i>
<i>Bipalium adventitium</i>	JL328	<a href="#">MZ561467</a>	15,494 bp	<i>cob</i>	–
<i>Bipalium kewense</i>	JL184A	<a href="#">MK455837</a>	15,666 bp	–	–

mitogenomes seemed complete, and all are colinear concerning protein-coding and rRNA genes. The situation with tRNA is slightly different. The number of tRNAs found among the mitogenomes varies between 21 to 22. For example, it was impossible to find a *tRNA-Thr* for both specimens of *H. covidum*, while it is commonly found in the cluster of tRNA comprised between *cob* and *rrnL* in other species such as *B. kewense*, *D. mayottensis* or *B. vagum*. Also, *B. adventitium* singularizes itself from the others by the total lack of tRNA cluster in the aforementioned area. Instead, two of these tRNAs, *tRNA-Asn* and *tRNA-Leu* were found in an intergenic area between *ND5* and *ND6*. In a similar situation to that explained below regarding the 16S gene, it should be noted that it was often difficult to detect tRNA among these specimens.

No putative *ATP8* gene could be evidenced so far. Blastx analyses of all mitogenomes from Bipaliinae were done against a customized database that included the putative *ATP8* amino-acid sequences of *Stenostomum sthenum* Borkott, 1970 ([ARW59252](#)) and *Macrostomum lignano* Ladurner, Schärer, Salvenmoser & Rieger 2005 ([ARW59249](#)) from [Egger, Bachmann & Fromm \(2017\)](#), and also the putative ORF neighbouring the *ND2* gene of *Girardia* sp. ([KP090061](#)) and *Phagocata gracilis* Haldeman, 1840 ([KP090060](#)), considered by [Ross et al. \(2016\)](#) as putative highly divergent *ATP8*. All attempts failed to find any *ATP8* candidate among the Bipaliinae.

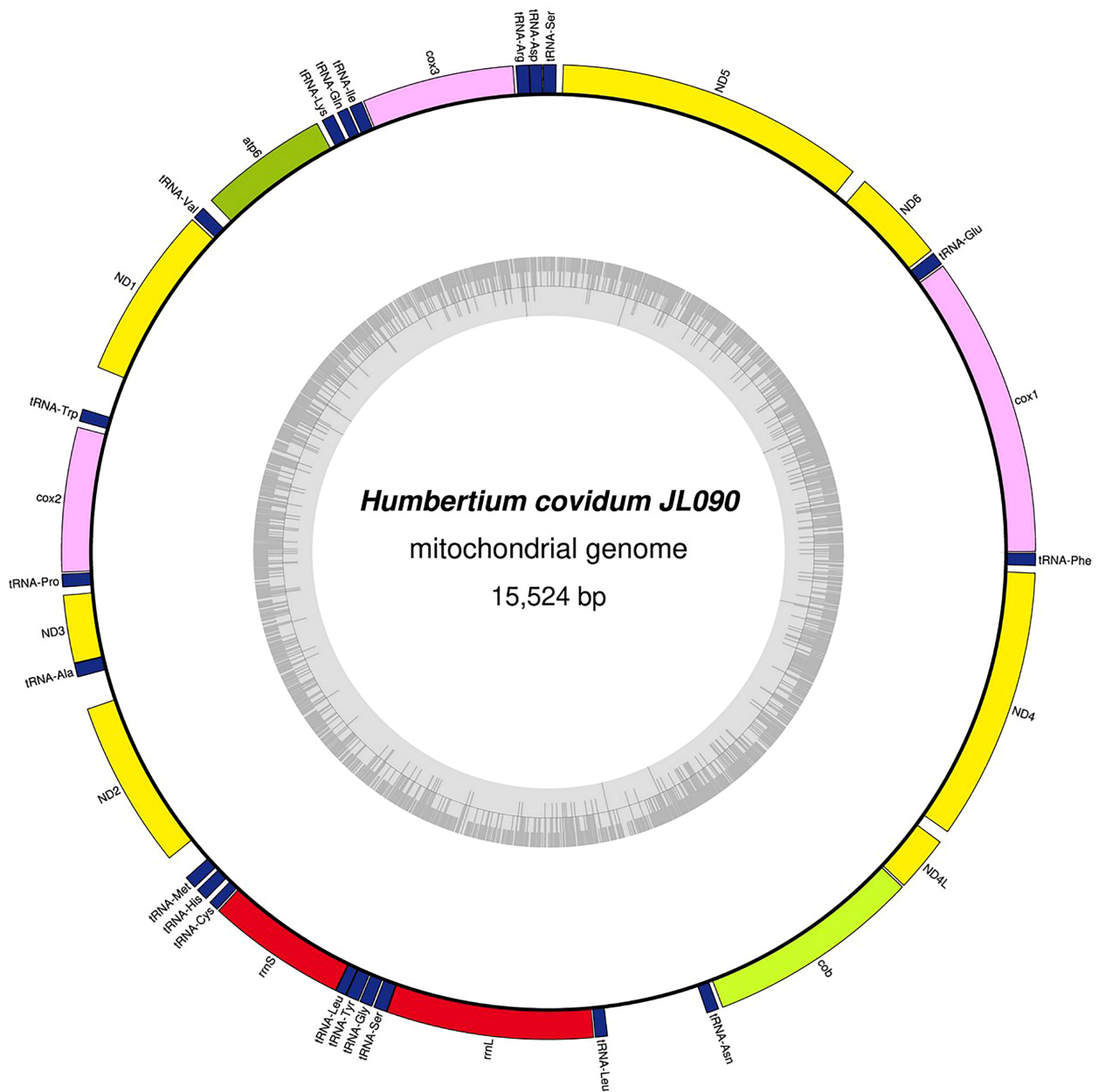
### Genomic comparison at the population level of *H. covidum*

[Table 4](#) lists the protein-coding genes of *H. covidum*, and compares the sequences obtained from JL351 (from Italy) and JL090 (from France). All mitochondrial protein-coding genes were found to display polymorphisms, some of them being non-silent. A gene commonly used for molecular barcoding and phylogeny such as the *cox1* gene showed 35 polymorphisms on 1,551 bp, which corresponds to a percentage of difference of 2.25%. This difference is interpreted as intraspecific. As a comparison, *cox1* alignment between *Dugesia japonica* Ichikawa & Kawakatsu, 1964 and *D. ryukyuensis* Kawakatsu, 1976 showed a much larger difference of 17.91%. Similarly, *B. kewense* showed 16.93% differences with *B. adventitium* and 15.7% with *B. vagum*. Noticeable differences, which include SNPs and indels, were found in the 16S rRNA genes of the two specimens of *H. covidum*, as described below.



- complex I (NADH dehydrogenase)
- complex III (ubichinol cytochrome c reductase)
- complex IV (cytochrome c oxidase)
- ATP synthase
- transfer RNAs
- ribosomal RNAs

**Figure 28** Mitogenome of *Humbertium covidum* n. sp.: genomic map of specimen MNHN JL351. Specimen from the Italian population in Casier. The mitogenome is 15,540 bp long and contains 12 protein coding genes, two ribosomal RNA genes and 21 transfer RNA genes. The ND3 gene was found with a premature stop codon. [Full-size DOI: 10.7717/peerj.12725/fig-28](https://doi.org/10.7717/peerj.12725/fig-28)



- complex I (NADH dehydrogenase)
- complex III (ubichinol cytochrome c reductase)
- complex IV (cytochrome c oxidase)
- ATP synthase
- transfer RNAs
- ribosomal RNAs

**Figure 29** Mitogenome of *Humbertium covidum* n. sp.: genomic map of specimen MNHN JL090. Specimen from the French population in Billère (Pyrénées-Atlantiques). The mitogenome is 15,524 bp long and contains 12 protein coding genes, two ribosomal RNA genes and 21 transfer RNA genes. The ND3 gene was found with a premature stop codon. [Full-size DOI: 10.7717/peerj.12725/fig-29](https://doi.org/10.7717/peerj.12725/fig-29)

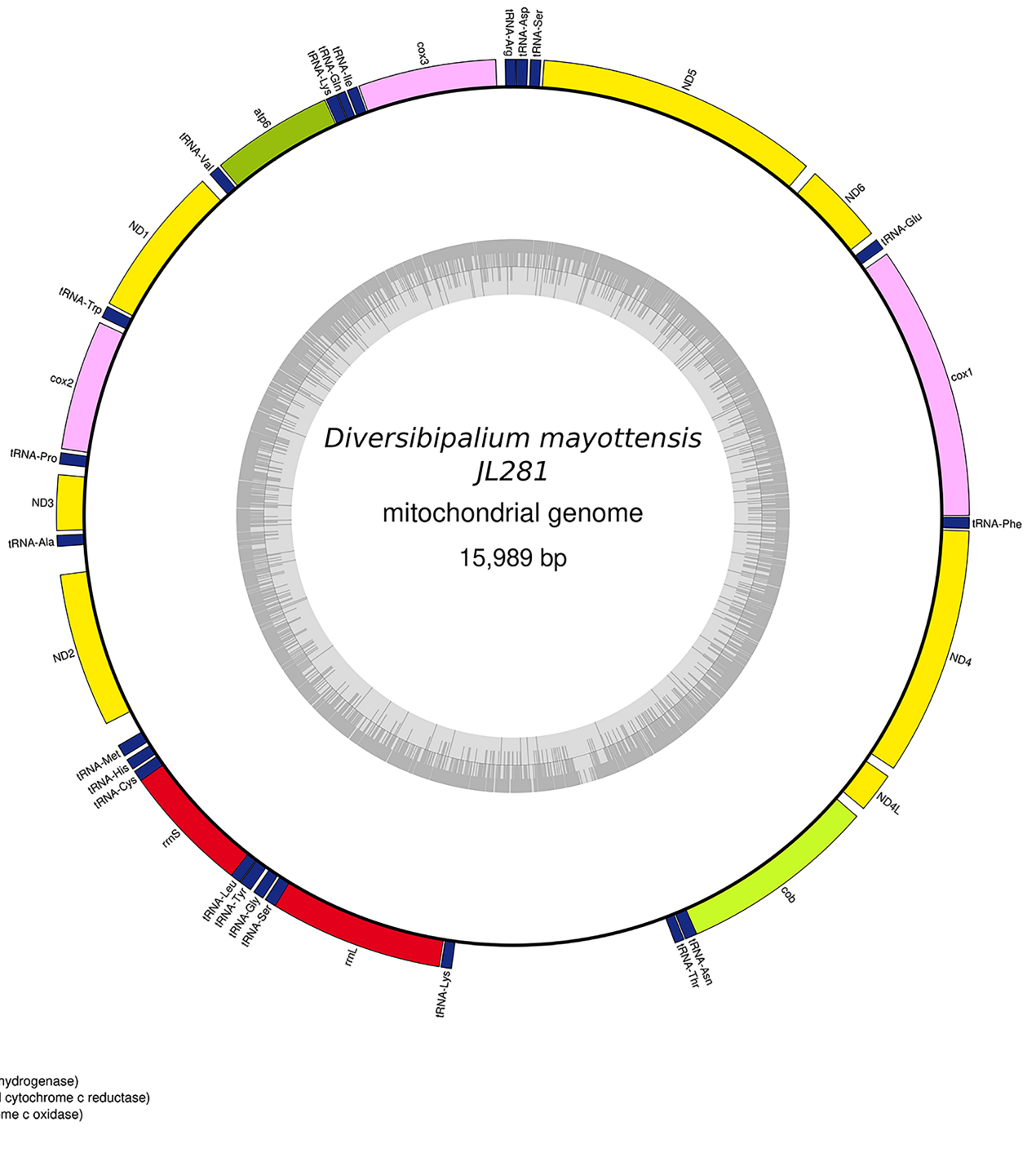
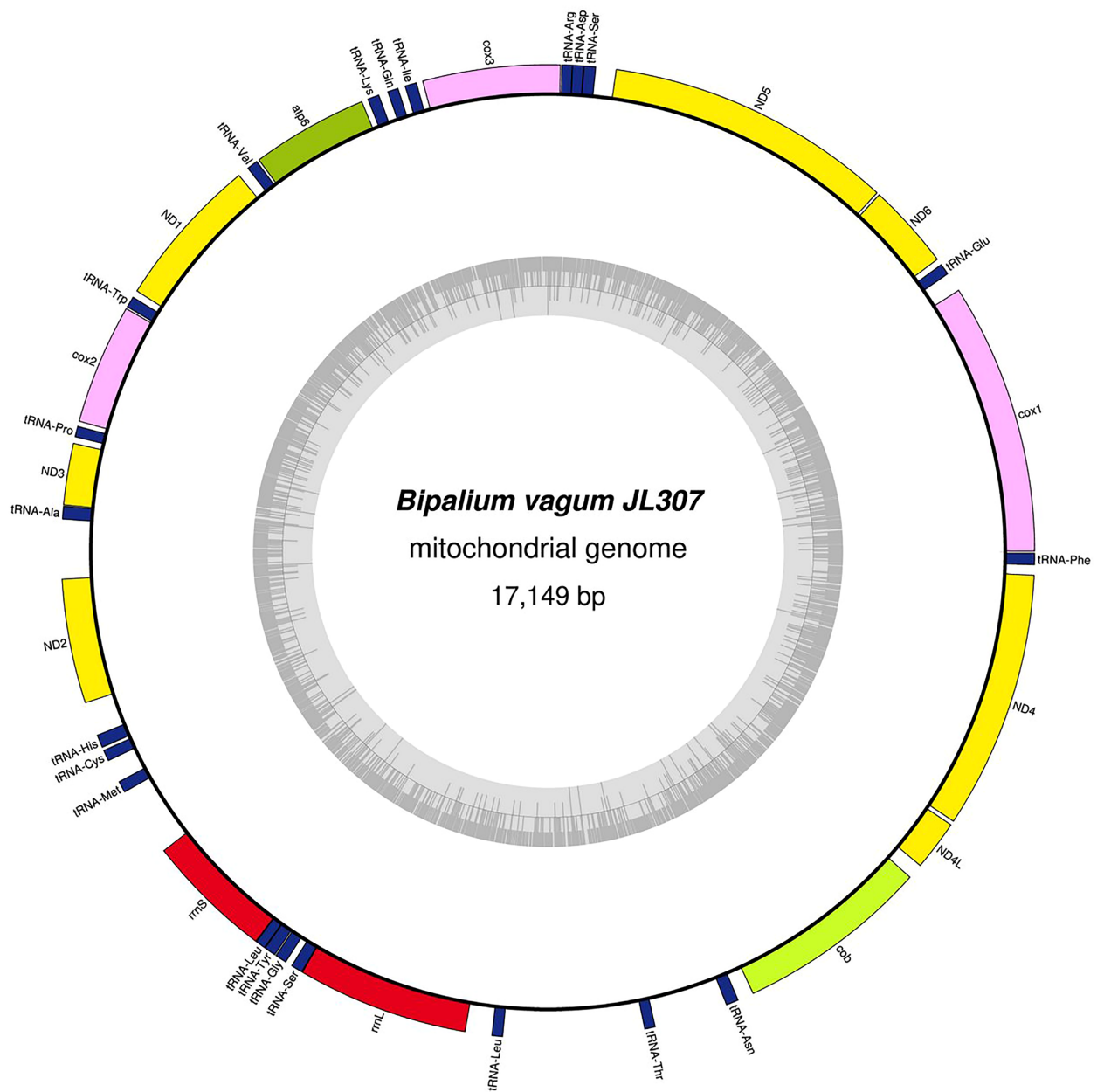


**Figure 30** Mitogenome of *Diversibipalium mayottensis* n. sp.: genomic map of specimen JL281. The mitogenome is 15,989 bp long and contains 12 protein coding genes, two ribosomal RNA genes and 22 transfer RNA genes. [Full-size !\[\]\(5fd6ef84f97f42d7f8b34275f1b65312\_img.jpg\) DOI: 10.7717/peerj.12725/fig-30](https://doi.org/10.7717/peerj.12725/fig-30)

### *The peculiar case of the 16S gene*

As more mitogenomes of Bipaliinae have been sequenced, a recurrent issue has arisen. Systematically, tools such as MITOS and MITOS2 were unable to locate the exact position



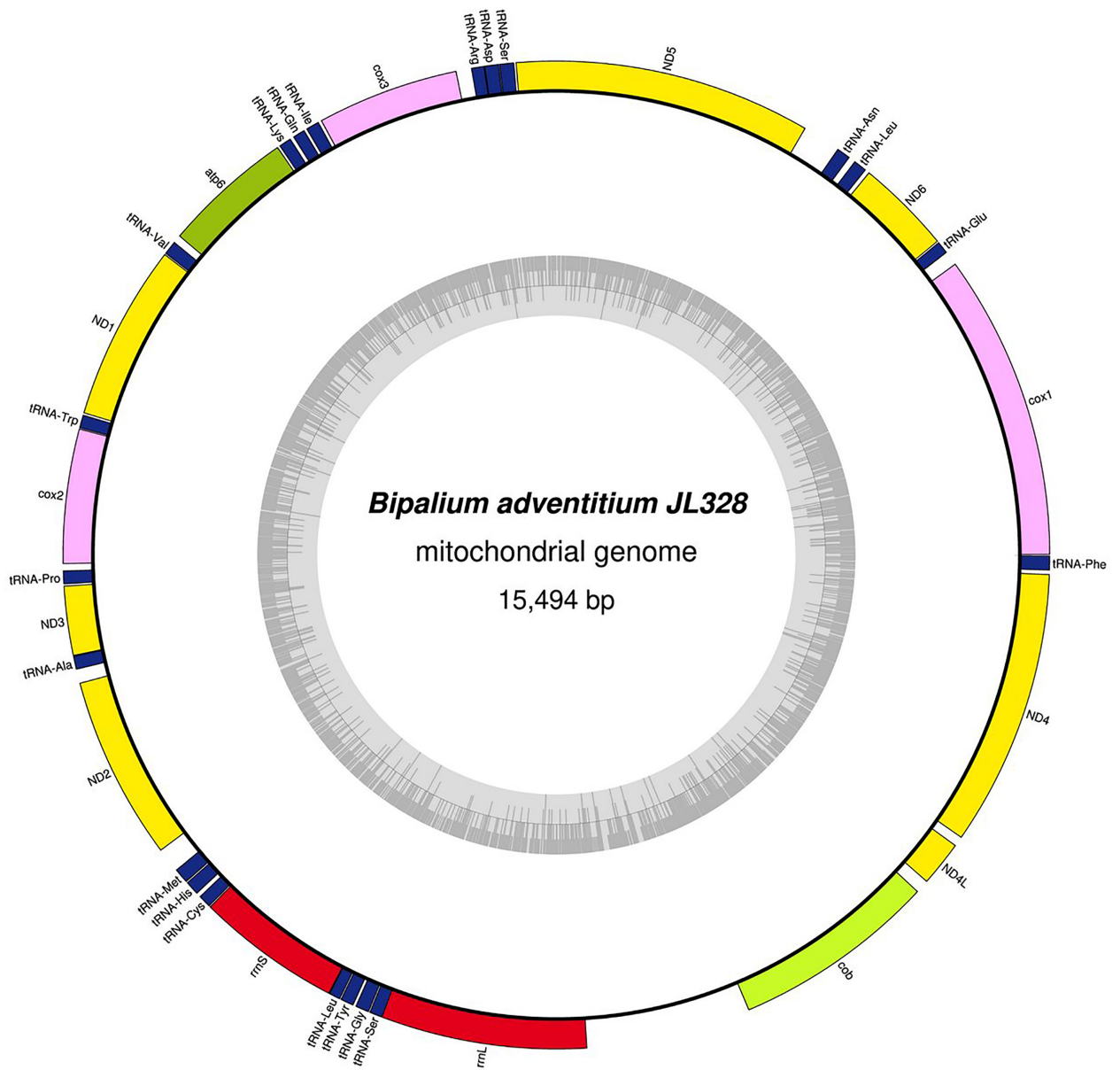


- complex I (NADH dehydrogenase)
- complex III (ubichinol cytochrome c reductase)
- complex IV (cytochrome c oxidase)
- ATP synthase
- transfer RNAs
- ribosomal RNAs

**Figure 31** Mitogenome of *Bipalium vagum*: genomic map of specimen JL307. The mitogenome is 17,149 bp long and contains 12 protein coding genes, two ribosomal RNA genes and 22 transfer RNA genes. The genes *cox3*, *atp6*, *ND1*, *ND4L* have alternative start codon.

Full-size DOI: [10.7717/peerj.12725/fig-31](https://doi.org/10.7717/peerj.12725/fig-31)

of the 16S gene. For example, when submitting the mitogenome of *H. covidum* JL351 to these software programmes, only a 563 bp fragment was recognised, meaning that a large subunit of the ribosome, which is smaller than the small subunit, is itself 726 bp long.



- complex I (NADH dehydrogenase)
- complex III (ubichinol cytochrome c reductase)
- complex IV (cytochrome c oxidase)
- ATP synthase
- transfer RNAs
- ribosomal RNAs

**Figure 32 Mitogenome of *Bipalium adventitium*: genomic map of specimen JL328.** The mitogenome is 15,494 bp long and contains 12 protein coding genes, two ribosomal RNA genes and 21 transfer RNA genes. It was not possible to find a stop codon for the *cob* gene.

Full-size DOI: [10.7717/peerj.12725/fig-32](https://doi.org/10.7717/peerj.12725/fig-32)

To verify the putative position of the 16S, additional alignments were performed with the reference sequence from *Schmidtea mediterranea* Benazzi, Baguña, Ballester, Puccinelli & Del Papa, 1975 ([JX398125](https://doi.org/10.1093/oxfordjournals.ima.a1000000)), which has the advantage of having been verified by



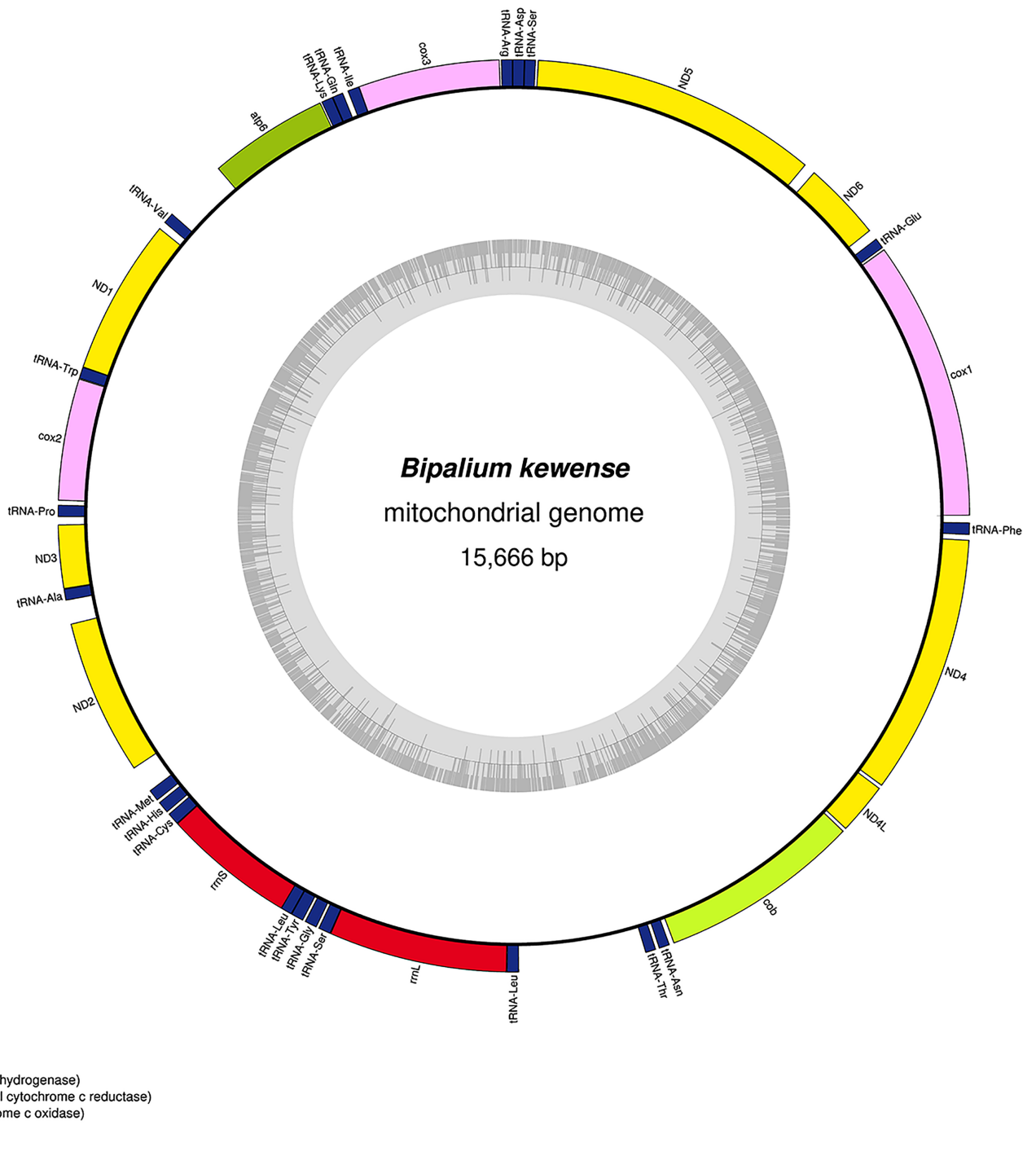
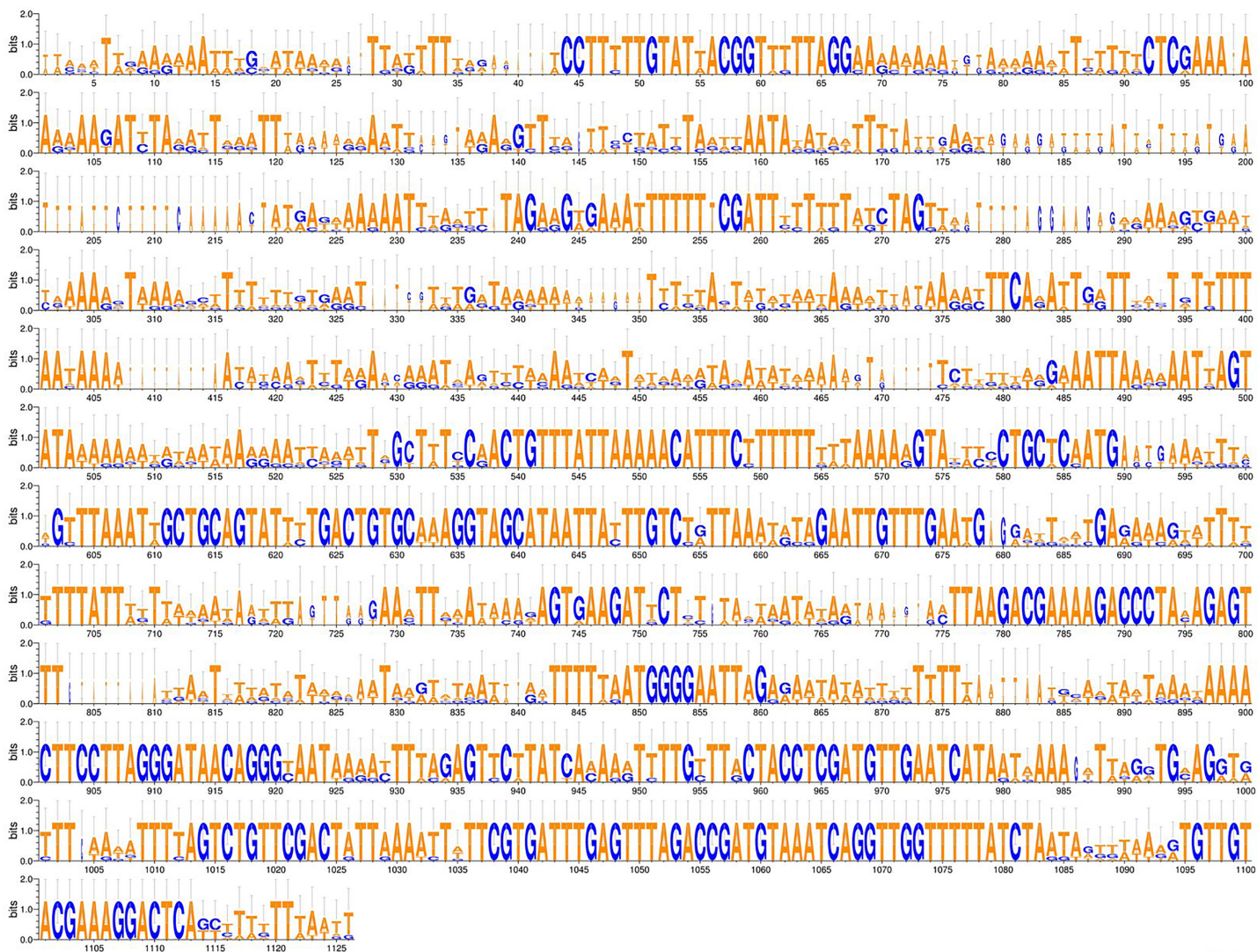


**Figure 34** Mitogenome of *Bipalium kewense*: genomic map of specimen JL184A. The mitogenome is 15,666 bp long and contains 12 protein coding genes, two ribosomal RNA genes and 22 transfer RNA genes. [Full-size !\[\]\(5f471a71b78d7676bc356df190b88ab4\_img.jpg\) DOI: 10.7717/peerj.12725/fig-34](https://doi.org/10.7717/peerj.12725/fig-34)

and in this case, it was associated with the main clade. The mitochondrial protein tree (Fig. 39) showed the highest support. In this tree, *H. covidum* was associated with *B. adventitium*. *Bipalium vagum* was again distinct from the main clade, but here with

**Table 4** Genetic differences between two populations (JL351, Italy vs JL090, France) of *Humbertium covidum*.

	<i>atp6</i>	<i>cob</i>	<i>cox1</i>	<i>cox2</i>	<i>cox3</i>	<i>ND1</i>	<i>ND2</i>	<i>ND3</i>	<i>ND4</i>	<i>ND4L</i>	<i>ND5</i>	<i>ND6</i>
Polymorphic site (nucleotides)	19/669	36/1,110	35/1,551	20/747	20/786	19/897	17/870	6/352	27/1,407	8/291	46/1,599	15/492
Percentage of differences (nucleotides)	2.84	3.24	2.25	2.68	2.54	2.19	1.95	1.70	1.92	2.75	2.88	3.05
Polymorphic sites (amino-acids)	8/222	7/369	3/516	4/248	1/261	7/298	4/289	2/117	4/468	3/96	11/532	7/163
Percentage of differences (amino-acids)	3.60	1.90	0.58	1.61	0.38	2.34	1.38	1.70	0.85	3.125	2.07	4.29



WebLogo 3.7.4

**Figure 35** An alignment of the 'complete' 16S genes from all Bipaliinae displayed as a LOGO. The alignment obtained from seven sequences representing six species shows the presence of a more conserved second part of the gene while the first part appears strongly variable.Full-size  DOI: 10.7717/peerj.12725/fig-35

100% support. Finally, the three-gene tree (Fig. 40) also associated *H. covidum* with *B. adventitium*, and both with *B. vagum*, but with lower ML node supports (65% and 59%, respectively), while BI node supports were higher (1.00 and 0.96, respectively).

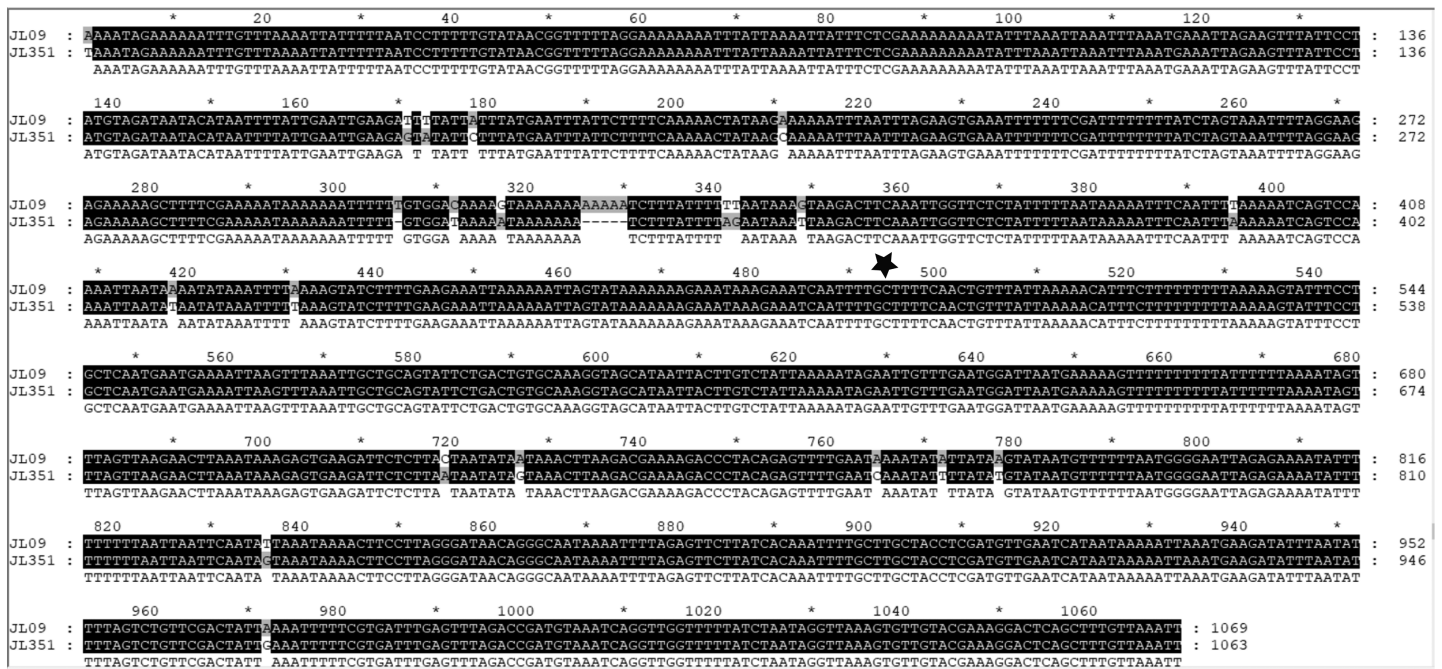


**Figure 36** Alignments of the ‘complete’ 16S genes from *H. covidum* JL090 and JL351. The two specimens are from the French (JL09) and Italian (JL351) populations. The black star indicates the beginning of the most conserved part evidenced by multispecies alignment.

Full-size DOI: 10.7717/peerj.12725/fig-36

The most noticeable difference between the concatenated trees was the relative position of the Geoplaninae and Rhynchodeminae. In the mitochondrial protein-coding genes tree (Fig. 39), Bipaliinae were associated with Rhynchodeminae with a node support of 62%, while Geoplaninae were distinguished from both with a node support of 100%. The three-gene tree (Fig. 40) associated Bipaliinae and Geoplaninae with node supports of 68% ML and 1.00 BI, while Rhynchodeminae were distinguished from both with a node support of 68% ML and 1.00 BI. It must be noted that for the three-gene phylogeny, the *cox1* partial gene only accounted for ca. 10% of the size of the trimmed concatenated sequences, since it had to include the partial genes of *N. venosum* and *B. nobile*, which were consequently shorter than the complete genes retrieved from full mitogenomes. Nonetheless, this difference in topology is intriguing, and would justify further investigations.

There was a constant and substantial result displayed by all phylogenies (Figs. 37–40), which is the position of *D. mayottensis*, always outside the main clade including all other Bipaliinae, with very high support. In contrast to *B. vagum* for example, whose position varied depending on the marker, *D. mayottensis* always appeared as a sister-group and relatively distant from a clade including all available representatives of *Humbertium*, *Bipalium*, *Novibipalium* and *Diversibipalium*. *Diversibipalium mayottensis* thus appeared to be the sister-group of all other bipaliines.

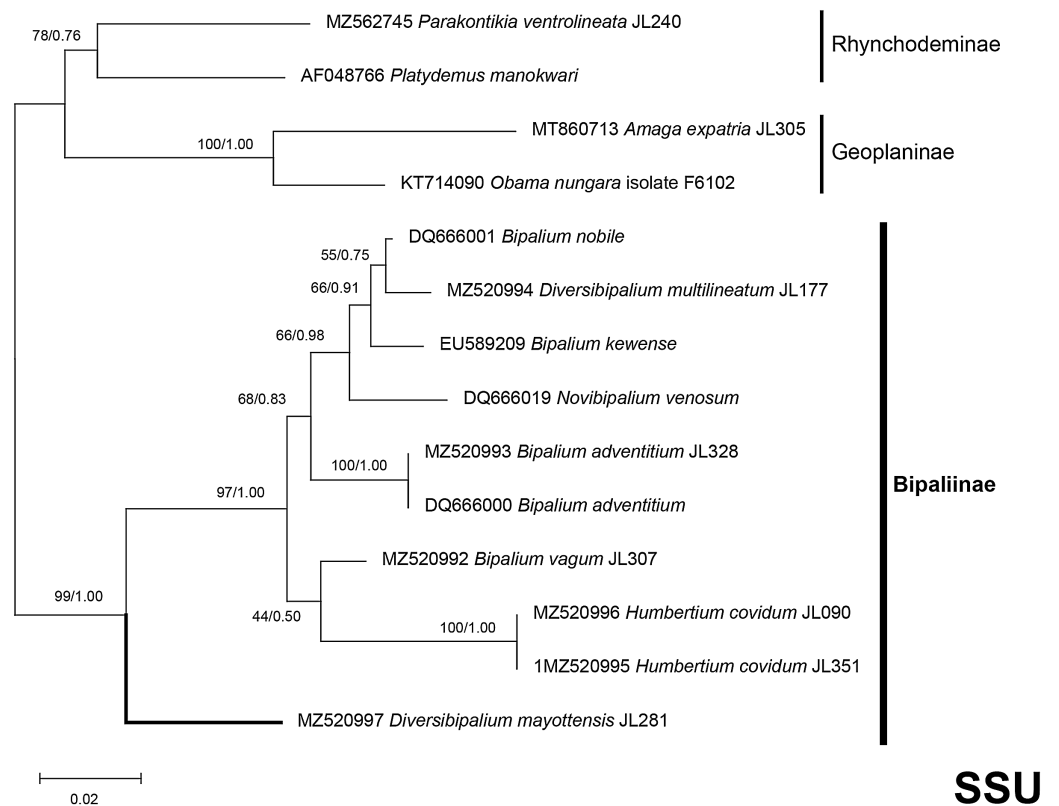


**Figure 37** SSU phylogenetic tree of bipaliine geoplanids. Maximum likelihood phylogenetic tree based on 14 partial SSU genes, using the GTR+I+G model of evolution, with the best tree out of 100 computed for 1,000 bootstrap replications. The tree with the best likelihood is shown ( $-2,551.353092$ ). ML bootstrap support values on the left. The BI tree had an identical topology, posterior probabilities are indicated on the right as decimal values. *Diversibipalium mayottensis* n. sp. appears as the sister-group to all other bipaliines. The subfamilies within the Geoplanidae (Rhynchodeminae, Geoplaninae and Bipaliinae) are indicated. *Diversibipalium mayottensis* branch in bold to show its position as sister-group to all other Bipaliinae. [Full-size !\[\]\(fd7fe780e8fd8eece60268c87d0c3e04\_img.jpg\) DOI: 10.7717/peerj.12725/fig-37](https://doi.org/10.7717/peerj.12725/fig-37)

### Alien DNA and prey

Positive results for alien DNA were obtained for *B. adventitium*, *B. vagum* and both specimens of *H. covidum*. All results are listed in [Table 5](#), and are available as [File S3](#) and discussed below.

Gastropod DNA was found among both specimens of *H. covidum*. Depending on the megablast results, some of these sequences could be linked with known species. Results obtained on *H. covidum* JL090 (from France) suggest that this specimen has been feeding on the garden slug *Arion hortensis* (A. Férussac, 1819) (Arionidae). There were also traces of DNA possibly originating from *Discus rotundatus* (O. F. Müller, 1774) (Discidae), a very small species of land snails, although here the megablasts are to be interpreted with more caution regarding their percentage of identity. For *H. covidum* JL351 (from Italy), most of the sequences found suggest that it has been feeding on *Cochlicopa lubrica* (O. F. Müller, 1774) (Cochlicopidae), another species of small land snail. Among others, a large contig corresponding to a complete, circular mitogenome was found by additional

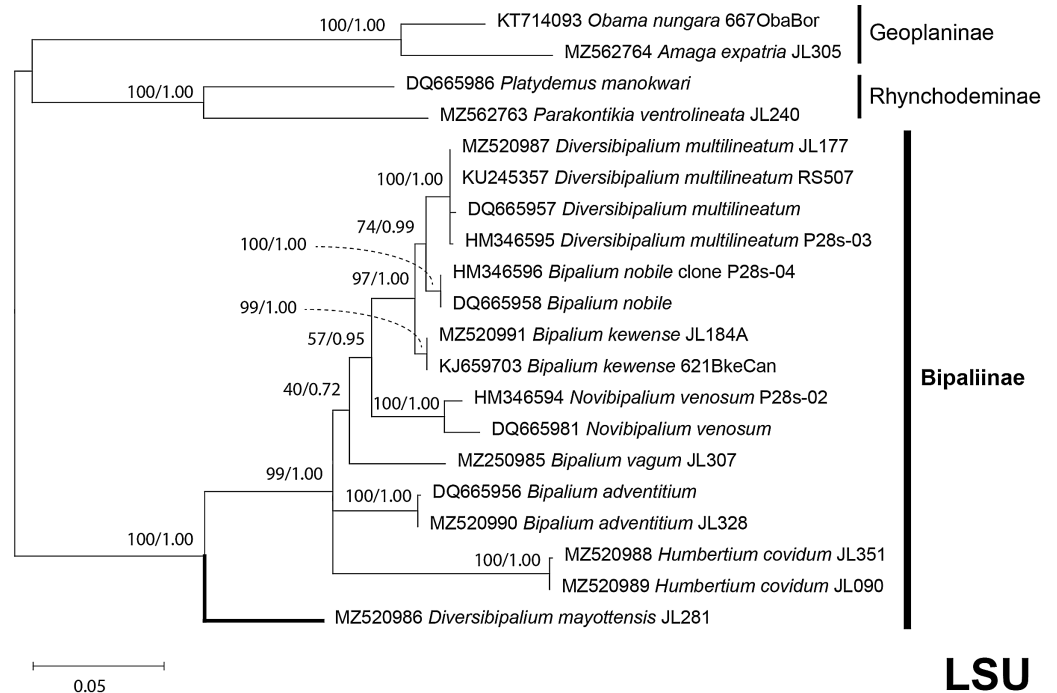


**Figure 38** LSU phylogenetic tree of bipaliine geoplanids. Maximum likelihood phylogenetic tree based on 20 partial LSU genes, using the GTR+I+G model of evolution, with the best tree out of 100 computed for 1,000 bootstrap replications. The tree with the best likelihood is shown ( $-4,759.571033$ ). ML bootstrap support values on the left. The BI tree had identical topology; posterior probabilities are indicated on the right as decimal values. The subfamilies within the Geoplanidae (Rhynchodeminae, Geoplaninae and Bipaliinae) are indicated. *Diversibipalium mayottensis* branch in bold to show its position as sister-group to all other Bipaliinae. Full-size [DOI: 10.7717/peerj.12725/fig-38](https://doi.org/10.7717/peerj.12725/fig-38)

data mining after retrieving its SSU. After trimming and extraction of its *cox1* gene, a megablast query returned 99.24% identity with [MF544766-Cochlicopa lubrica](#). For *B. adventitium* JL328, we found traces of a Lumbricidae. Finally, *B. vagum* JL307 (from Guadeloupe) had traces of DNA probably originating from *Subulina octona* (Bruguière, 1789) (Achatinidae) or *Subulina striatella* (Rang, 1831), two snail species widespread in the Caribbean.

## DISCUSSION

### The new species *Humbertium covidum*

#### *Molecular results: cox1 sequences of specimens from three localities*

The partial *cox1* sequences of the three specimens from the two localities in France were identical, suggesting that they belong to the same population. The two localities (Saint-Pée-sur-Nivelle and Billère) are distant by about 100 km. The *cox1* sequences of all 6 specimens from Italy (a single locality) were identical. The partial *cox1* sequences of the Italian specimens were different from the French specimens by 2.58%. We consider that these differences are intraspecific, and that the same species was involved in both localities (Fig. 1). A longer discussion is provided below, based on complete mitogenome sequences.



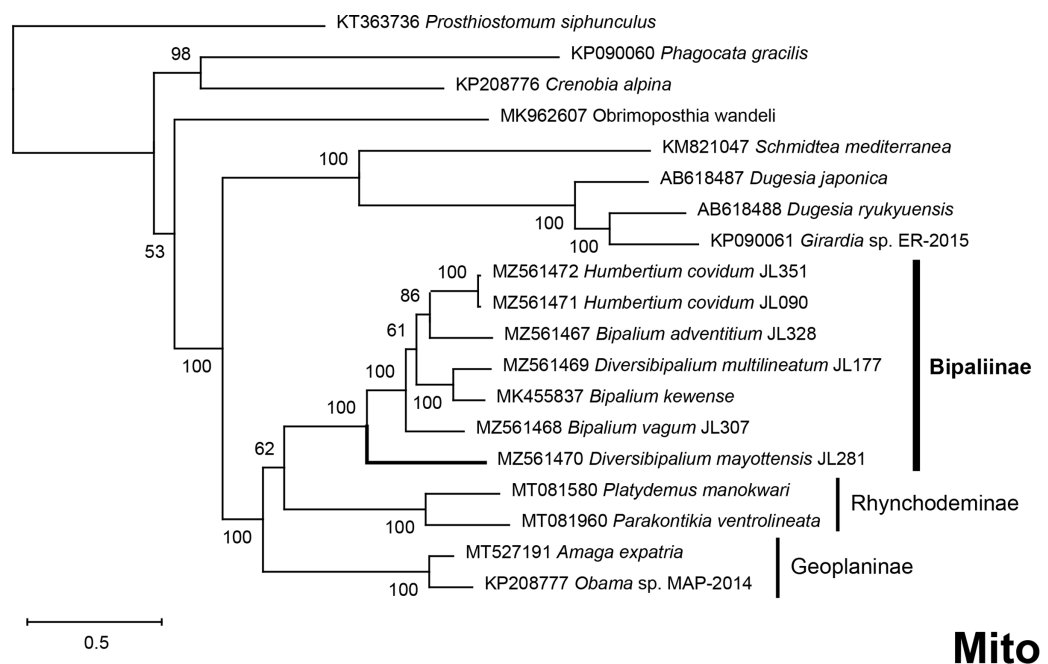


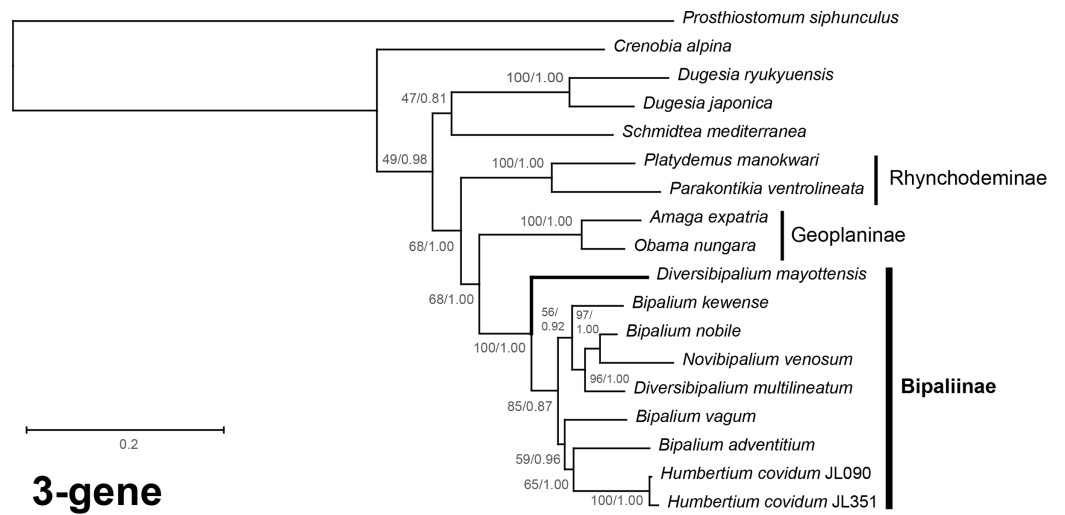
**Figure 39** Phylogenetic tree of concatenated mitochondrial proteins of bipaliine geoplanids. Maximum likelihood phylogenetic tree based on concatenated protein sequences extracted from 19 mitogenomes using the mtART+I+G model, with the best tree out of 100 computed for 1,000 bootstrap replications. The tree with the best likelihood is shown ( $-4,759.571033$ ). The subfamilies within the Geoplanidae (Rhynchodeminae, Geoplaninae and Bipaliinae) are indicated. *Diversibipalium mayottensis* branch in bold to show its position as sister-group to all other Bipaliinae.

Full-size  DOI: [10.7717/peerj.12725/fig-39](https://doi.org/10.7717/peerj.12725/fig-39)

### Morphology and systematics

The genus *Humbertium* was erected ([Ogren & Sluys, 2001](#)) to accommodate species (23 species stated but only 22 listed) with the single apomorphic condition OVD-1 in which the ovovitelline ducts turn dorsally before reaching the gonopore and having an antero-dorsal entrance to the female organ, the proflex condition. Currently, of the 22 species of *Humbertium*, excluding *H. covidum*, three species (*H. ferrugineoideum* ([Sabussowa, 1925](#)), *H. sikori* ([von Graff, 1899](#)), and *H. palmisium* ([de Beauchamp, 1930](#))) are uncertain as the OVD-1 character is not clearly shown in figures or mentioned in the text ([Ogren & Sluys, 2001](#)). Only three species are well described: *H. ceres* ([Moseley, 1875](#)), *H. ravenalae* ([von Graff, 1899](#)), and *H. woodworthi* ([von Graff, 1899](#)), the descriptions of the remainder being too concise, or mostly confined to the external morphology and the anatomy of the copulatory organs.

The type-species of *Humbertium* is *Perocephalus ravenalae* [von Graff, 1899](#). Externally, *H. covidum* mainly differs from this species with its brown-black to black dorsal ground colour and lacking dorsal stripes (*H. ravenalae* has a brownish dorsal ground colour with fine paired dark median stripe either side of a pale median stripe that passes onto the black headplate, and fine paired dark marginal stripes). The length of *H. ravenalae* is some three times that of *H. covidum*, and the body apertures are more posteriorly displaced. The internal anatomy of *H. ravenalae* was described by [Mell \(1903; von Graff, 1899\)](#).



### 3-gene

**Figure 40** Three-gene phylogenetic tree of bipaliine geoplanids, based on concatenated *cox1*, SSU and LSU genes. Maximum likelihood phylogenetic tree based on 18 concatenated partial sequences of *cox1*, SSU and LSU, using the GTR+I+G model of evolution, with the best tree out of 100 computed for 1,000 bootstrap replications. The tree with the best likelihood is shown (−24,779.059136). ML bootstrap support values on the left. The BI tree had identical topology; posterior probabilities are indicated on the right as decimal values. The subfamilies within the Geoplanidae (Rhynchodeminae, Geoplaninae and Bipaliinae) are indicated. *Diversibipalium mayottensis* branch in bold to show its position as sister-group to all other Bipaliinae. Full-size DOI: 10.7717/peerj.12725/fig-40

**Table 5** Alien DNA detected in the samples.

Sample and geographic origin	Contig size (in bp)	Coverage	Best blastn results (organism, accession number, E-value, identity)
<i>H. covidum</i> JL090 Billère, France	5,953	87.595262	<i>Arion hortensis</i> , KU341315, 0.0, 99.19%
	2,209	20.638418	<i>Discus rotundatus</i> , FJ917212, 0.0, 98.28%
	2,150	2.882324	<i>Arion hortensis</i> , MG856341, 0.0, 99.77%
	1,624	72.587394	<i>Discus rotundatus</i> , FJ917212, 0.0, 95.57%
<i>H. covidum</i> JL351 Casier, Italy	14,281	3.216540	<i>Cochlicopa lubrica</i> ( <i>cox1</i> only), MF544766, 0.0, 99.24%
	2,140	93.634550	<i>Cochlicopa lubrica</i> , AY014019, 0.0, 99.23%
	633	136.802920	<i>Cochlicopa lubrica</i> , GU331944, 0.0, 99.84%
	413	113.274390	<i>Oxychilus alliarius</i> , MN022707, 0.0, 97.64%
<i>B. adventitium</i> JL328 Montréal, Québec, Canada	312	125.061674	Various gastropods
	9,730	52.980923	<i>Eisenia foetida</i> , AF212166, 0.0, 98.87%
<i>B. vagum</i> JL307 Morne Vert, Martinique	5,994	7.978338	<i>Subulina octona</i> , MF444887, 0.0, 99.97%
	3,025	22.415306	<i>Subulina striatella</i> , MN022690, 0.0, 99.66%

*Humbertium covidum* shares the same pharyngeal musculature and pharynx type as *H. ravenalae*, the general musculature of the copulatory organs, and the near vertical placement of the female glandular canal, though in *H. ravenalae* the proximal female canal tilts anteriad, while in *H. covidum* it tilts slightly posteriad. A viscid gland and common genital canal of the type in *H. covidum* and *H. ceres* are absent in *H. ravenalae*.

In the two specimens of *Humbertium covidum* examined histologically, the ovovitelline ducts turn dorsally before the gonopore (holotype) and at the posterior lip of the gonopore (paratype), rise and enter the female glandular canal antero-dorsally. Despite the slight difference between the two specimens at the point at which the ovovitelline ducts begin to ascend, attributed here to relative differences in maturity, the antero-dorsal entrance of these ducts into the female canal are present in both specimens, and it is considered that they exhibit the OVD-1 condition that characterises species of the genus *Humbertium*.

Within the genus *Humbertium*, *H. covidum* is a small species about 20 mm long, readily differentiated externally from the only other described and considerably larger black species, *H. ferrugineoideum* (*Sabussowa, 1925*) from Madagascar, which attains a length of 75–80 mm, and is black both dorsally and ventrally (*H. covidum* is grey to greyish brown ventrally), with a white margin of the anterior headplate that is absent in *H. covidum*. Internally, the penis and female glandular canal of *H. ferrugineoideum* are both acutely angled ventrad some 20° from the vertical (the penis bulb is almost horizontal in *H. covidum*), the glandular canal is not thistle-shaped as in *H. covidum*, and there is no viscid gland (present in *H. covidum*).

Externally, plain brown-black to black *H. covidum* is distinguished from similar small “black” species. These include *Diversibipalium piceum* (*von Graff, 1897* in *von Graff, 1899*) from central Sulawesi, that is 43 mm long (preserved) black with blueish stippling dorsally and ventrally with black creeping sole, and well developed lappets on the headplate (*H. covidum* has a reniform headplate without lappets, without blue stippling and with a pale brownish-grey to grey creeping sole). Similar small “black” species also include *D. smithi* (*von Graff, 1899*) from Darjeeling, northern India, 54 mm long (preserved) with velvety blueish black dorsum with a touch of dull brown, and yellowish-rusty brown colour ventrally with a deep cream-yellowish creeping sole demarcated with blueish-light green margins (*von Graff, 1899, Whitehouse, 1914*) (*H. covidum* lacks a blueish cast to the dorsal ground colour and has a pale brownish grey to grey creeping sole that is not demarcated as in *D. smithi*). Two other much larger species with dark brown to black ground colour are *D. richtersi* (*von Graff, 1899*) from Madagascar, 94 mm long (preserved) with a small head with weakly formed lappets, dark brown dorsally and ventrally, grading to a reddish colour under the headplate, and mouth displaced more posteriorly than in *H. covidum*, and *D. kirckpatricki* from Sri Lanka, 60 mm long (preserved), dark brown dorsally and ventrally, with a pale creeping sole, but with strongly recurved lappets as in *D. falcatum* from Sumatra, and mouth displaced more posteriorly than in *H. covidum*. There is also an alien black molluscivorous *Diversibipalium* species, some 110+ mm long (living) with rounded lappets and small brownish headplate, and possibly with a black median dorsal stripe, recorded in and around Durban in South Africa (Himansu Baijnath pers.com to LW 2016 and observations #35482045, #37914997 and #61592889 in iNaturalist); the species is considered too large to be *H. covidum*.

The specimens with external morphology nearest to *H. covidum* are the *Diversibipalium* sp. “Kumamoto” of *Yamamoto (2000)* from Japan that is 30 mm long, dark brown-black in colour with an indistinct dark mid-dorsal stripe (*Yamamoto, 2000*). However, the

**Table 6** *Humbertium covidum*: possible occurrence worldwide.

Locality, Country	Comments	Date	Reference	C/ P
Saint-Pée-sur-Nivelle, France		2013	<i>Justine et al., 2018</i>	C
Billère, France		2019	This paper	C
Casier, Province of Treviso, Italy		2019	This paper	C
Kumamoto, Kyushu Island, Japan		2000	<i>Kawakatsu, Sluys &amp; Ogren, 2005</i>	P
Marina di Cerveteri, Province of Rome, Italy	Photographs from Citizen Science	2014	<i>Mori et al., 2022</i>	P
Likander peninsula, Popov Island, Eugénie Archipelago, off Russia, Sea of Japan	Based on their Fig. 3	2017	<i>Prozorova &amp; Ternovenko, 2018</i>	P
Xiamen, Chinese coast facing Taiwan strait, P. R. China	iNaturalist observation	2018	Observation #19171303	P
Xiamen, P. R. China	iNaturalist observation	2018	Observation #19171787	P
Petrov Bay, Lazovsky Nature Reserve, Primorye Territory, Russia	Based on her Fig. 2A	2019	<i>Prozorova, 2021</i>	
Hachijō-jima Island, Philippines Sea, off Japan main islands	Based on their Fig. 2	unknown	<i>Meyer-Rochow &amp; Miinalainen, 2020</i>	P

**Notes:**

The table provides a list of *possible* occurrences based on similarity of external morphology. All these records need to be confirmed, especially by molecular methods. C/P: C, confirmed with molecular data; P, possible, based on photographs.

dorsal aspect of a living specimen of *H. covidum* is indistinguishable in photographs from that of an undescribed species of *Diversibipalium* from Xiamen, China (see Table 6 for iNaturalist data).

Internally, with regard to the anatomy of the copulatory organs, in particular the morphology of the proximal female glandular canal, the unusual common genital canal, and presence of a viscid gland, *Humbertium covidum* stands closest to *Humbertium ceres* (*Moseley, 1875*), originally described from specimens collected in the Royal Botanic Gardens, Peradeniya near Kandy, Sri Lanka (*Moseley, 1875*), with the internal anatomy subsequently described by *von Graff (1899)*.

Externally, a preserved specimen of *H. ceres* measures 79 mm in length, with mouth 52 mm (65.8% of body length), and gonopore 64 mm (81% of body length), both displaced more posteriorly than in *H. covidum*. In addition, the dorsum of *H. ceres* is divisible into five longitudinal stripes, the whole of the dorsal aspect of the planarian is irregularly speckled in black, and the headplate is ornamented in dark and light bands. The ventral surface is characterised by paired slight sub-marginal glandular ridges.

Internally, the copulatory organs of *H. ceres* share with *H. covidum* an unusual development of the genital pad creating a broad, narrow elongate common genital duct. At the anterior end of the duct in *H. ceres* is what von Graff terms a uterus (*von Graff, 1899*). A similar structure, identified here from its secretions as a viscid gland, is present in the anterior genital pad at the end of the common genital duct in *H. covidum*; it is highly likely the “uterus” of *H. ceres* is also a viscid gland. The thistle-shaped proximal end of the female glandular canal in *H. covidum* is similar to the shape of the seminal receptacle at the proximal end of the glandular canal in *H. ceres*. However, the seminal receptacle in *H. ceres* does not receive shell gland secretions, and the ovovitelline ducts

open into the glandular canal below the receptacle. In *H. covidum*, the ovovitelline ducts enter the invaginated dorsal end of the proximal glandular canal that receives shell gland secretions. The major difference between these two species is the anteriorly prolapsed female glandular canal in *H. ceres*, characteristic of a group of three species in *Humbertium*: *H. ceres*, *H. proserpina* and *H. woodworthi* that all exhibit this feature (character FCA-2 (Ogren & Sluys, 1998)), absent in *H. covidum* in which the female glandular canal is almost vertical with a slight posteriad tilt.

The viscid gland in *H. covidum* is characterised by cyanophil secretions and appears analogous to the viscid glands described in species of Rhynchodemini and Caenoplanini (Winsor, 1998a; Winsor, 1998b). It differs from the musculoglandular organs described by Müller (Müller, 1902) in *Bipalium graffi* and *B. bohmi* (Type III of Winsor (Winsor, 1998a)) that discharge erythrophil secretions into the common atrium. These musculoglandular organs are situated on the genital bulge and appear analogous to the adenchyma on the atrial flaps of species of *Artioposthia* in which they have been demonstrated to have a role in cocoon formation (Winsor, 1998a).

### **Occurrences in Europe and possible occurrences in Asia**

As mentioned above, the species has been found in two widely separated gardens in the Department of Pyrénées-Atlantiques in the South-West of France, and one locality in the Province of Treviso in North-Eastern Italy. However, it is well known that bipaliine species are most numerous in South East Asia and Madagascar (von Graff, 1899); we found in the literature and citizen science databases a few records that might be the same species (Table 6). Most localities in Asia appear to be on islands or coastal areas, but the database is certainly extremely incomplete.

*Humbertium covidum* is probably a species originating from Asia and is an alien species in Europe. Whether it will become an invasive species needs to be monitored in the future.

### **The new species *Diversibipalium mayottensis***

#### **Morphology**

There are no other bipaliine planarians described with the blue-green iridescent dorsal ground colour observed in *D. mayottensis*. Similar iridescence, which is lost on fixation, has been observed in various species of Caenoplanini, and is possibly due to tightly packed transparent proteinaceous rhabdoids in the epithelium, acting as a diffraction grating (Winsor, 2003).

With regard to the club-shaped headplate and general body shape, *D. mayottensis* is similar to the general morphology of species of *Humbertium*. In particular, *D. mayottensis* shares the relative positions of the body apertures with the mouth present in the anterior second fifth of the body, and gonopore in the fourth body fifth, with two species: *H. woodworthi* (von Graff, 1899) with four dark dorsal stripes, from Madagascar, and *H. subboreale* (Sabussowa, 1925) a small dark brown species from China.

#### **Molecular characteristics**

In 2018 we wrote: “The COI barcode of this specimen is clearly different from all other known sequences. We can safely claim that this species has never been sequenced before”

(Justine et al., 2018). Our current results on the complete mitogenome confirm that the species is distinct from all other species for which the mitogenome is known; in addition, *D. mayottensis* was sister-group to all other bipaliines in all our phylogenetic analyses. This is probably more significant than the superficial morphological resemblance with various *Humbertium* species mentioned above.

### **Possible origin of the species**

Because of the proximity of Mayotte with Madagascar, it may be hypothesized that the origin of the species is Madagascar, not Asia as for most Bipaliinae.

### **Mitogenomes**

Including *B. kewense* (Gastineau et al., 2019), there are now up to 6 species of Bipaliinae for which mitogenomes have been sequenced. For some of them, there were a few protein-coding genes for which it was not possible to find either start or stop codons. There are already several reports among Platyhelminthes of mitochondrial protein-coding genes for which no start codon could be found (Justine et al., 2020a; Ross et al., 2016; Sakai & Sakaizumi, 2012; Solà et al., 2015). In the case of *H. covidum*, the *ND3* gene is supposed to have a premature stop, by addition at the 3' extremity of two A after a T, immediately followed by the *tRNA-Ala*. No stop codon or premature stop could be found at all for the *cob* gene of *B. adventitium* JL328, for reasons that remain unknown. Excluding *D. multilineatum* because of its incompleteness, it is possible to say that most of these species have mitogenomes of a size similar to *B. kewense* (ca. 15,500 bp), with *D. mayottensis* being slightly longer (15,989 bp). The main exception is *B. vagum*, whose mitogenome is 17,149 bp long. *Bipalium vagum* also had the highest number of alternative start codons, with four protein-coding genes concerned (*cox3*, *atp6*, *ND1*, *ND4L*). This extra-length seems to be explained by large intergenic sections located between the 16S and *cob* genes, where the three conserved tRNA (*tRNA-Leu*, *tRNA-Thr*, and *tRNA-Asn*) are separated from each other by hundreds of base pairs. We could not circularise the mitogenome of *D. multilineatum*, even after several iterations of Consed's 'addSolexaReads' function. This suggests that this lacking region consists of repeated sequences that short-read sequencing technologies fail to reveal. We underline the fact that this missing part is located at the very same position as the extra length in *B. vagum*'s mitogenome.

We would also like to indicate that recent investigations on parasitic flatworms such as *Echinococcus granulosus* Batsch, 1786, *Clonorchis sinensis* Loos, 1907 and *Schistosoma haematobium* (Bilharz, 1852) using long-read technologies have shown considerable extra-lengths within these mitogenomes, as much as 18.5 kb long (Kinkar et al., 2021; Kinkar et al., 2019; Kinkar et al., 2020). We tend to think that in the near future, long-read technologies might unveil similar features among Geoplanidae.

### **Alien DNA and diet**

Our results on alien DNA suggest that *H. covidum* feeds on slugs and snails, with a very clear result concerning *Cochlicopa lubrica* in Italy; this is the only information currently available concerning the diet of this new species. The information was based on a small

number of specimens and should be confirmed by additional experiments. Results on *B. adventitium* (from Canada) suggest that the specimen fed on a lumbricid earthworm, a result compatible with other information on the diet of the species (Ducey et al., 1999). For *B. vagum* JL307 from Guadeloupe, results suggest that the specimen fed on a species of *Subulina*, a small snail; the species is known to feed on snails (Ducey, McCormick & Davidson, 2007). Interestingly, similar studies on *Amaga expatria*, an alien geoplanid found in Martinique, another island in the Caribbean, also found that it fed on species of *Subulina* (Justine et al., 2020a); species of *Subulina* are widespread in the Caribbean (Delannoie et al., 2015).

### A distinct genus for *Diversibipalium mayottensis*?

All phylogenies showed *D. mayottensis* as a sister-group to all other Bipaliinae, thus confirming its appurtenance to the subfamily, but making it impossible to assign it to any of the known genera of bipaliines. The subfamily currently includes four genera, namely *Bipalium*, *Humbertium*, *Novibipalium* Kawakatsu et al., 1998 and the collective genus *Diversibipalium*. External morphology superficially suggests that the species is close to *Humbertium*, but the reproductive anatomy is unknown. Its position as sister-group to all other bipaliines suggests that a new genus should be described to accommodate *D. mayottensis*. We refrain from doing so here in the absence of anatomical information.

## CONCLUSION

In this paper, we formally described two species of bipaliine geoplanids, previously only known as unnamed species included in the collective genus *Diversibipalium*. For the first species, *Humbertium covidum* n. sp., we subsequently obtained fresh specimens collected in Italy and could fully describe the anatomy, based on histological methods. This was not possible for the second species, found only on Mayotte, which is described here as *Diversibipalium mayottensis* n. sp. on the basis of external morphology. We newly characterised the complete mitochondrial genome of five species of bipaliine geoplanids, including the two new species and *B. adventitium*, *B. vagum* and *D. multilineatum*. Based on phylogenetic analyses of the SSU, LSU, mitochondrial proteins and concatenated *cox1*-SSU-LSU, we built phylogenies of bipaliines for which these sequences are available (6 species). In all phylogenies, *D. mayottensis* was the sister-group of all other bipaliines, suggesting that it represents a distinct genus, which needs formal description; this will await availability of additional specimens. Furthermore, we demonstrated that next generation sequencing methods provide an excellent tool for delineating and describing species of geoplanids, since they allow access to both traditionally used sequences (SSU, LSU and *cox1*) and complete mitochondrial genomes which provide considerable additional information.

## ABBREVIATIONS USED IN FIGURES OF HISTOLOGY

af	atrial flap
ca	common atrium
cc	copulatory canal

<b>cgc</b>	common genital canal
<b>ch</b>	chondrocytes
<b>clm</b>	cutaneous longitudinal muscles
<b>cm</b>	cutaneous musculature
<b>cs</b>	ciliated creeping sole
<b>dfg</b>	distal female glandular canal (= vagina)
<b>dip</b>	dorsal insertion of pharynx
<b>dtm</b>	dorsal transverse muscles
<b>ed</b>	ejaculatory duct
<b>eg</b>	erythrophil glands
<b>pfg</b>	proximal female glandular canal
<b>g</b>	gonopore
<b>gm</b>	glandular mesenchyme
<b>gp</b>	genital pad
<b>i</b>	intestine
<b>ma</b>	male atrium
<b>m</b>	mouth
<b>nc</b>	nerve cord
<b>ovd</b>	ovovitelline duct
<b>pb</b>	penis bulb-penis
<b>pg</b>	penial glands
<b>ph</b>	pharynx
<b>php</b>	pharyngeal pouch
<b>pp</b>	penis papilla
<b>sd</b>	spermiducal vesicle
<b>sg</b>	shell glands
<b>sr</b>	seminal receptacle
<b>sv</b>	seminal vesicle
<b>te</b>	testis
<b>tm</b>	transverse parenchymal muscle
<b>vd</b>	vas deferens
<b>vg</b>	viscid gland
<b>vi</b>	vitellaria
<b>vip</b>	ventral insertion of pharynx
<b>vp</b>	ventral muscle plate

## ACKNOWLEDGEMENTS

We thank the colleagues and people who provided specimens, especially Mathieu Coulis, Mathieu Théry, Geneviève Rolland-Martinez and Dino Carraro. We emphasize that



lockdowns and social distancing helped us to concentrate on completion of this paper, but we will not forget that the pandemic has affected and still affects the world terribly—the Latin epithet *covidum* for our new species should thus be considered a homage to the victims of the COVID-19 pandemic.

## ADDITIONAL INFORMATION AND DECLARATIONS

### Funding

This work was supported by several grants (ATM) from the Muséum National d'Histoire Naturelle, Paris, France. The funders had no role in study design, data collection and analysis, decision to publish, or preparation of the manuscript.

### Grant Disclosures

The following grant information was disclosed by the authors:  
Muséum National d'Histoire Naturelle, Paris, France.

### Competing Interests

Jean-Lou Justine is an Academic Editor of PeerJ.

### Author Contributions

- Jean-Lou Justine conceived and designed the experiments, performed the experiments, analyzed the data, prepared figures and/or tables, authored or reviewed drafts of the paper, obtained funding, coordinated collective effort, and approved the final draft.
- Romain Gastineau conceived and designed the experiments, performed the experiments, analyzed the data, prepared figures and/or tables, authored or reviewed drafts of the paper, performed bioinformatics on mitogenomes and phylogenetic analyses, and approved the final draft.
- Pierre Gros performed the experiments, prepared figures and/or tables, made photographs of living animals, and approved the final draft.
- Delphine Gey performed the experiments, authored or reviewed drafts of the paper, performed Sanger sequencing, and approved the final draft.
- Enrico Ruzzier performed the experiments, prepared figures and/or tables, authored or reviewed drafts of the paper, collected worms, made a movie, and approved the final draft.
- Laurent Charles performed the experiments, prepared figures and/or tables, authored or reviewed drafts of the paper, collected worms, made photographs, and approved the final draft.
- Leigh Winsor conceived and designed the experiments, performed the experiments, analyzed the data, prepared figures and/or tables, authored or reviewed drafts of the paper, performed histology, made drawings and photographs, and approved the final draft.

## DNA Deposition

The following information was supplied regarding the deposition of DNA sequences:

The sequences are available at GenBank:

MG655588, MZ520996, MZ622153, MZ622148–MZ622152, MZ647546–MZ647548, MZ520988, MZ520995, MG655598, MG655596, MG655597, MG655599, MZ561467–MZ561472.

## Data Availability

The following information was supplied regarding data availability:

The six following sequences (complete mitogenomes) are available in the [Supplemental File](#) and at GenBank: [MZ561467–MZ561472](#).

The partial sequences from “alien” DNA (DNA from preys) are available in the [Supplemental File](#).

## New Species Registration

The following information was supplied regarding the registration of a newly described species:

Publication LSID: urn:lsid:zoobank.org:pub:27A4D685-9042-40C2-A40A-89FF8BCC489B.

*Humbertium covidum* n. sp.

urn:lsid:zoobank.org:act:3847E9FE-463B-4FDB-A164-88765A52D65A.

*Diversibipalium mayottensis* n. sp.

urn:lsid:zoobank.org:act:B59FEE8E-70FD-4DEC-B839-554C351701F8.

## Supplemental Information

Supplemental information for this article can be found online at <http://dx.doi.org/10.7717/peerj.12725#supplemental-information>.

## REFERENCES

- Abascal F, Posada D, Zardoya R. 2007. MtArt: a new model of amino acid replacement for Arthropoda. *Molecular Biology and Evolution* **24**(1):1–5 DOI [10.1093/molbev/msl136](https://doi.org/10.1093/molbev/msl136).
- Andújar C, Creedy TJ, Arribas P, López H, Salces-Castellano A, Pérez-Delgado AJ, Vogler AP, Emerson BC. 2021. Validated removal of nuclear pseudogenes and sequencing artefacts from mitochondrial metabarcode data. *Molecular Ecology Resources* **21**(6):1772–1787 DOI [10.1111/1755-0998.13337](https://doi.org/10.1111/1755-0998.13337).
- Bankevich A, Nurk S, Antipov D, Gurevich AA, Dvorkin M, Kulikov AS, Lesin VM, Nikolenko SI, Pham S, Prjibelski AD. 2012. SPAdes: a new genome assembly algorithm and its applications to single-cell sequencing. *Journal of Computational Biology* **19**(5):455–477 DOI [10.1089/cmb.2012.0021](https://doi.org/10.1089/cmb.2012.0021).
- Bernt M, Donath A, Jühling F, Externbrink F, Florentz C, Fritsch G, Pütz J, Middendorf M, Stadler PF. 2013. MITOS: improved de novo metazoan mitochondrial genome annotation. *Molecular Phylogenetics and Evolution* **69**(2):313–319 DOI [10.1016/j.ympev.2012.08.023](https://doi.org/10.1016/j.ympev.2012.08.023).
- Boratyn GM, Schäffer AA, Agarwala R, Altschul SF, Lipman DJ, Madden TL. 2012. Domain enhanced lookup time accelerated BLAST. *Biology Direct* **7**(1):12 DOI [10.1186/1745-6150-7-12](https://doi.org/10.1186/1745-6150-7-12).

- Buhay JE. 2009.** “COI-like” sequences are becoming problematic in molecular systematic and DNA barcoding studies. *Journal of Crustacean Biology* **29**:96–110 DOI [10.1651/08-3020.1](https://doi.org/10.1651/08-3020.1).
- Capella-Gutiérrez S, Silla-Martínez JM, Gabaldón T. 2009.** trimAl: a tool for automated alignment trimming in large-scale phylogenetic analyses. *Bioinformatics* **25**:1972–1973 DOI [10.1093/bioinformatics/btp348](https://doi.org/10.1093/bioinformatics/btp348).
- Carbayo F, Alvarez-Presas M, Jones HD, Riutort M. 2016.** The true identity of *Obama* (Platyhelminthes: Geoplanidae) flatworm spreading across Europe. *Zoological Journal of the Linnean Society* **177**:5–28 DOI [10.1111/zoj.12358](https://doi.org/10.1111/zoj.12358).
- Carranza S, Littlewood DTJ, Clough KA, Ruiz-Trillo I, Bagaña J, Riutort M. 1998.** A robust molecular phylogeny of the Tricladida (Platyhelminthes: Seriata) with a discussion on morphological synapomorphies. *Proceedings of the Royal Society of London B* **265**:631–640 DOI [10.1098/rspb.1998.0341](https://doi.org/10.1098/rspb.1998.0341).
- Crooks GE, Hon G, Chandonia J-M, Brenner SE. 2004.** WebLogo: a sequence logo generator. *Genome Research* **14**:1188–1190 DOI [10.1101/gr.849004](https://doi.org/10.1101/gr.849004).
- Darriba D, Taboada GL, Doallo R, Posada D. 2012.** jModelTest 2: more models, new heuristics and parallel computing. *Nature Methods* **9**:772 DOI [10.1038/nmeth.2109](https://doi.org/10.1038/nmeth.2109).
- Delannoye R, Charles L, Pointier J-P, Massemin D. 2015.** *Mollusques continentaux de la Martinique*. Paris: Muséum national d’Histoire naturelle.
- Ducey PK, McCormick M, Davidson E. 2007.** Natural history observations on *Bipalium* cf. *vagum* Jones and Sterrer (Platyhelminthes: Tricladida), a terrestrial broadhead planarian new to North America. *Southeastern Naturalist* **6**:449–461 DOI [10.1656/1528-7092\(2007\)6\[449:NHOBC\]2.0.CO;2](https://doi.org/10.1656/1528-7092(2007)6[449:NHOBC]2.0.CO;2).
- Ducey PK, Messere M, Lapoint K, Noce S. 1999.** Lumbricid prey and potential herpetofaunal predators of the invading terrestrial flatworm *Bipalium adventitium* (Turbellaria: Tricladida: Terricola). *American Midland Naturalist* **141**:305–314 DOI [10.1674/0003-0031\(1999\)141\[0305:LPAPHP\]2.0.CO;2](https://doi.org/10.1674/0003-0031(1999)141[0305:LPAPHP]2.0.CO;2).
- Ducey PK, West L-J, Shaw G, De Lisle J. 2005.** Reproductive ecology and evolution in the invasive terrestrial planarian *Bipalium adventitium* across North America. *Pedobiologia* **49**:367–377 DOI [10.1016/j.pedobi.2005.04.002](https://doi.org/10.1016/j.pedobi.2005.04.002).
- Egger B, Bachmann L, Fromm B. 2017.** *Atp8* is in the ground pattern of flatworm mitochondrial genomes. *BMC Genomics* **18**:414 DOI [10.1186/s12864-017-3807-2](https://doi.org/10.1186/s12864-017-3807-2).
- Froehlich EM. 1955.** Sobre espécies brasileiras do gênero *Geoplana*. *Boletim da Faculdade de Filosofia, Ciências e Letras da Universidade de São Paulo, Série Zoologia* **19**:289–339 DOI [10.11606/issn.2526-3382.bffclzoologia.1954.120096](https://doi.org/10.11606/issn.2526-3382.bffclzoologia.1954.120096).
- Gastineau R, Justine J-L. 2020.** Complete mitogenome of the invasive land flatworm *Parakontikia ventrolineata*, the second Geoplanidae (Platyhelminthes) to display an unusually long *cox2* gene. *Mitochondrial DNA Part B* **5**:2115–2116 DOI [10.1080/23802359.2020.1765709](https://doi.org/10.1080/23802359.2020.1765709).
- Gastineau R, Justine J-L, Lemieux C, Turmel M, Witkowski A. 2019.** Complete mitogenome of the giant invasive hammerhead flatworm *Bipalium kewense*. *Mitochondrial DNA Part B* **4**:1343–1344 DOI [10.1080/23802359.2019.1596768](https://doi.org/10.1080/23802359.2019.1596768).
- Gastineau R, Lemieux C, Turmel M, Justine J-L. 2020.** Complete mitogenome of the invasive land flatworm *Platydemus manokwari*. *Mitochondrial DNA Part B* **5**:1689–1690 DOI [10.1080/23802359.2020.1748532](https://doi.org/10.1080/23802359.2020.1748532).
- Glez-Peña D, Gómez-Blanco D, Reboiro-Jato M, Fdez-Riverola F, Posada D. 2010.** ALTER: program-oriented conversion of DNA and protein alignments. *Nucleic Acids Research* **38**(Web Server issue):W14–W18 DOI [10.1093/nar/gkq321](https://doi.org/10.1093/nar/gkq321).

- Gordon D, Abajian C, Green P. 1998.** Consed: a graphical tool for sequence finishing. *Genome Research* 8:195–202 DOI 10.1101/gr.8.3.195.
- Graham NR, Gillespie RG, Krehenwinkel H. 2021.** Towards eradicating the nuisance of numts and noise in molecular biodiversity assessment. *Molecular Ecology Resources* 21:1755–1758 DOI 10.1111/1755-0998.13414.
- Hasegawa M, Kishino H, Yano T. 1985.** Dating the human-ape split by a molecular clock of mitochondrial DNA. *Journal of Molecular Evolution* 22:160–174 DOI 10.1007/BF02101694.
- Hazkani-Covo E, Zeller RM, Martin W. 2010.** Molecular poltergeists: mitochondrial DNA copies (numts) in sequenced nuclear genomes. *PLoS Genetics* 6(2):e1000834 DOI 10.1371/journal.pgen.1000834.
- Hlaing T, Tun-Lin W, Somboon P, Socheat D, Setha T, Min S, Chang MS, Walton C. 2009.** Mitochondrial pseudogenes in the nuclear genome of *Aedes aegypti* mosquitoes: implications for past and future population genetic studies. *BMC Genetics* 10:11 DOI 10.1186/1471-2156-10-11.
- Hyman LH. 1943.** Endemic and exotic land planarians in the United States: with a discussion of necessary changes of names in the Rhynchodemidae. *American Museum Novitates* 1–21.
- Jones HD, Sterrer W. 2005.** Terrestrial planarians (Platyhelminthes, with three new species) and nemertines of Bermuda. *Zootaxa* 1001:31–58 DOI 10.11646/zootaxa.1001.1.3.
- Justine J-L, Gey D, Thévenot J, Gastineau R, Jones HD. 2020a.** The land flatworm *Amaga expatria* (Geoplanidae) in Guadeloupe and Martinique: new reports and molecular characterization including complete mitogenome. *PeerJ* 8:e10098 DOI 10.7717/peerj.10098.
- Justine J-L, Gey D, Thévenot J, Gouraud C, Winsor L. 2020b.** First report in France of *Caenoplana decolorata*, a recently described species of alien terrestrial flatworm (Platyhelminthes, Geoplanidae). Available at <https://www.biorxiv.org/content/10.1101/2020.11.06.371385v1?rss=1>.
- Justine J-L, Gey D, Vasseur J, Thévenot J, Coulis M, Winsor L. 2021.** Presence of the invasive land flatworm *Platydemus manokwari* (Platyhelminthes, Geoplanidae) in Guadeloupe, Martinique and Saint Martin (French West Indies). *Zootaxa* 4951:381–390 DOI 10.11646/zootaxa.4951.2.11.
- Justine J-L, Théry T, Gey D, Winsor L. 2019.** First record of the invasive land flatworm *Bipalium adventitium* (Platyhelminthes, Geoplanidae) in Canada. *Zootaxa* 4656:591–595 DOI 10.11646/zootaxa.4656.3.13.
- Justine J-L, Thévenot J, Winsor L. 2014.** Les sept plathelminthes invasifs introduits en France. *Phytoma* 674:28–32 DOI 10.6084/m9.figshare.1447202.v1.
- Justine J-L, Winsor L, Barrière P, Fanai C, Gey D, Han AWK, La Quay-Velazquez G, Lee BPY-H, Lefevre J-M, Meyer J-Y, Philippart D, Robinson DG, Thévenot J, Tsatsia F. 2015.** The invasive land planarian *Platydemus manokwari* (Platyhelminthes, Geoplanidae): records from six new localities, including the first in the USA. *PeerJ* 3:e1037 DOI 10.7717/peerj.1037.
- Justine J-L, Winsor L, Gey D, Gros P, Thévenot J. 2014.** The invasive New Guinea flatworm *Platydemus manokwari* in France, the first record for Europe: time for action is now. *PeerJ* 2:e297 DOI 10.7717/peerj.297.
- Justine J-L, Winsor L, Gey D, Gros P, Thévenot J. 2018.** Giant worms *chez moi!* Hammerhead flatworms (Platyhelminthes, Geoplanidae, *Bipalium* spp., *Diversibipalium* spp.) in metropolitan France and overseas French territories. *PeerJ* 6:e4672 DOI 10.7717/peerj.4672.
- Justine J-L, Winsor L, Gey D, Gros P, Thévenot J. 2020c.** *Obama chez moi!* The invasion of metropolitan France by the land planarian *Obama nungara* (Platyhelminthes, Geoplanidae). *PeerJ* 8:e8385 DOI 10.7717/peerj.8385.

- Kalvari I, Nawrocki EP, Ontiveros-Palacios N, Argasinska J, Lamkiewicz K, Marz M, Griffiths-Jones S, Toffano-Nioche C, Gautheret D, Weinberg Z. 2021.** Rfam 14: expanded coverage of metagenomic, viral and microRNA families. *Nucleic Acids Research* **49**:D192–D200 DOI [10.1093/nar/gkaa1047](https://doi.org/10.1093/nar/gkaa1047).
- Katoh K, Standley DM. 2013.** MAFFT multiple sequence alignment software version 7: improvements in performance and usability. *Molecular Biology and Evolution* **30**:772–780 DOI [10.1093/molbev/mst010](https://doi.org/10.1093/molbev/mst010).
- Kawakatsu M, Ogren RE, Froehlich EM, Sasaki G-Y. 2002.** Additions and corrections of the previous land planarian indices of the world (Turbellaria, Seriata, Tricladida, Terricola). Additions and corrections of the previous land planarian indices of the world – 10. *Bulletin of the Fuji Women's College (Series 2)* **40**:157–177.
- Kawakatsu M, Sluys R, Ogren RE. 2005.** Seven new species of land planarian from Japan and China (Platyhelminthes, Tricladida, Bipaliidae), with a morphological review of all Japanese bipaliids and a biogeographic overview of Far Eastern species. *Belgian Journal of Zoology* **135**:53–77.
- Kinkar L, Gasser RB, Webster BL, Rollinson D, Littlewood DTJ, Chang BCH, Stroehlein AJ, Korhonen PK, Young ND. 2021.** Nanopore sequencing resolves elusive long tandem-repeat regions in mitochondrial genomes. *International Journal of Molecular Sciences* **22**:1811 DOI [10.3390/ijms22041811](https://doi.org/10.3390/ijms22041811).
- Kinkar L, Korhonen PK, Cai H, Gauci CG, Lightowlers MW, Saarma U, Jenkins DJ, Li J, Li J, Young ND. 2019.** Long-read sequencing reveals a 4.4 kb tandem repeat region in the mitogenome of *Echinococcus granulosus* (sensu stricto) genotype G1. *Parasites & Vectors* **12**:1–7 DOI [10.1186/s13071-019-3492-x](https://doi.org/10.1186/s13071-019-3492-x).
- Kinkar L, Young ND, Sohn W-M, Stroehlein AJ, Korhonen PK, Gasser RB. 2020.** First record of a tandem-repeat region within the mitochondrial genome of *Clonorchis sinensis* using a long-read sequencing approach. *PLOS Neglected Tropical Diseases* **14**:e0008552 DOI [10.1371/journal.pntd.0008552](https://doi.org/10.1371/journal.pntd.0008552).
- Kumar S, Stecher G, Tamura K. 2016.** MEGA7: molecular evolutionary genetics analysis version 7.0 for bigger datasets. *Molecular Biology and Evolution* **33**:1870–1874 DOI [10.1093/molbev/msw054](https://doi.org/10.1093/molbev/msw054).
- Lago-Barcia D, Fernández-Álvarez FA, Negrete L, Brusa F, Damborenea C, Grande C, Noreña C. 2015.** Morphology and DNA barcodes reveal the presence of the non-native land planarian *Obama marmorata* (Platyhelminthes: Geoplanidae) in Europe. *Invertebrate Systematics* **29**:12–22 DOI [10.1071/IS14033](https://doi.org/10.1071/IS14033).
- Lang A. 1884.** Die Polycladen (Seeplanarien) des Golfes von Neapel und der angrenzenden Meeresabschnitte. Leipzig: Engelmann.
- Laslett D, Canbäck B. 2008.** ARWEN, a program to detect tRNA genes in metazoan mitochondrial nucleotide sequences. *Bioinformatics* **24**:172–175 DOI [10.1093/bioinformatics/btm573](https://doi.org/10.1093/bioinformatics/btm573).
- Leite LA. 2012.** Mitochondrial pseudogenes in insect DNA barcoding: differing points of view on the same issue. *Biota Neotropica* **12**:301–308 DOI [10.1590/S1676-06032012000300029](https://doi.org/10.1590/S1676-06032012000300029).
- Lohse M, Drechsel O, Kahlau S, Bock R. 2013.** OrganellarGenomeDRAW—a suite of tools for generating physical maps of plastid and mitochondrial genomes and visualizing expression data sets. *Nucleic Acids Research* **41**:W575–W581 DOI [10.1093/nar/gkt289](https://doi.org/10.1093/nar/gkt289).
- Makino N, Shirasawa Y. 1983.** Morphological and ecological comparison with two new species of elongated slender land planarians have several stripes and their new scientific names [sic]. *Bulletin of Tokyo Medical College* **9**:69–83 [In Japanese, English summary].

- Makino N, Shirasawa Y. 1986.** Biology of long slender land planarians (Turbellaria) in Tokyo and environs. *Hydrobiologia* 132:229–232 DOI 10.1007/978-94-009-4810-5\_32.
- Mateos E, Jones HD, Riutort M, Álvarez-Presas M. 2020.** A new species of alien terrestrial planarian in Spain: *Caenoplana decolorata*. *PeerJ* 8:e10013 DOI 10.7717/peerj.10013.
- Mell C. 1903.** Die Landplanarien der Madagassischen Subregion. *Abhandlungen der Senckenbergischen Naturforschenden Gesellschaft* 239:193–236.
- Meyer-Rochow VB, Miinalainen I. 2020.** Squid sucker teeth and cocoons of a terrestrial flatworm: amino acid content of two nano-structurally identical tissues in phylogenetically unrelated taxa. *Zoology* 140:125798 DOI 10.1016/j.zool.2020.125798.
- Mori E, Giulia M, Panella M, Montagna M, Winsor L, Justine J-L, Menchetti M, Schifani E, Melone B, Mazza G. 2022.** Opening Pandora's box: the invasion of alien flatworms in Italy. *Biological Invasions* 24:205–216 DOI 10.1007/s10530-021-02638-w.
- Moseley HN. 1875.** V. On the anatomy and histology of the land-planarians of Ceylon, with some account of their habits, and a description of two new species, and with notes on the anatomy of some European aquatic species. *Philosophical Transactions of the Royal Society* 164:105–171 DOI 10.1098/rstl.1874.0005.
- Moseley HN. 1878.** Description of a new species of land-planarian from the hothouses at Kew Gardens. *Annals and Magazine of Natural History* 1:237–239 DOI 10.1080/00222937808682324.
- Müller J. 1902.** Ein Beitrag zur Kenntnis der Bipaliiden. *Zeitschrift für Wissenschaftliche Zoologie* 73:75–114.
- Nicholas KB, Nicholas HB Jr, Deerfield DW II. 1997.** GeneDoc: analysis and visualization of genetic variation. *EMBnet news* 4:14.
- Ogren RE. 1987.** Description of a new three-lined land planarian of the genus *Bipalium* (Turbellaria: Tricladida) from Pennsylvania, USA. *Transactions of the American Microscopical Society* 106:21–30 DOI 10.2307/3226281.
- Ogren RE, Sheldon JK. 1991.** Ecological observations on the land planarian *Bipalium pennsylvanicum* Ogren, with references to phenology, reproduction, growth rate and food niche. *Journal of the Pennsylvania Academy of Science* 65:3–9.
- Ogren RE, Sluys R. 1998.** Selected characters of the copulatory organs in the land planarian family Bipaliidae and their taxonomic significance (Tricladida: Terricola). *Hydrobiologia* 383:77–82 DOI 10.1023/A:1003417712473.
- Ogren RE, Sluys R. 2001.** The genus *Humbertium* gen. nov., a new taxon of the land planarian family Bipaliidae (Tricladida, Terricola). *Belgian Journal of Zoology* 131:201–204.
- Prozorova LA. 2021.** Новые находки молотоголовых планарий (Platyhelminthes: Tricladida: Continenticola: Bipaliinae) на российском Дальнем Востоке [New findings of hammerhead planarians (Platyhelminthes: Tricladida: Continenticola: Bipaliinae) on the Russian Far East]. *Biota and Environment of Natural Areas* 55–64 DOI 10.37102/2782-1978\_2021\_1\_4.
- Prozorova LA, Ternovenko VA. 2018.** Редкие и новые виды организмов Дальневосточного морского заповедника. 2. Наземные планарии (Platyhelminthes: Tricladida: Continenticola) [Rare and new species from the Far Eastern Marine Reserve. 2. Land Planarians (Platyhelminthes: Tricladida: Continenticola)]. *Biota and Environment* 3:54–59.
- Ronquist F, Teslenko M, van der Mark P, Ayres DL, Darling A, Höhna S, Larget B, Liu L, Suchard MA, Huelsenbeck JP. 2012.** MrBayes 3.2: efficient Bayesian phylogenetic inference and model choice across a large model space. *Systematic Biology* 61:539–542 DOI 10.1093/sysbio/sys029.

- Ross E, Blair D, Guerrero-Hernández C, Alvarado AS. 2016. Comparative and transcriptome analyses uncover key aspects of coding-and long noncoding RNAs in flatworm mitochondrial genomes. *G3: Genes, Genomes, Genetics* 6:1191–1200 DOI 10.1534/g3.116.028175.
- Sabussowa Z. 1925. Drei neue arten von landplanarien. *Zoologische Jahrbücher (Systematik)* 50:283–298.
- Sakai M, Sakaizumi M. 2012. The complete mitochondrial genome of *Dugesia japonica* (Platyhelminthes; order Tricladida). *Zoological Science* 29:672–680 DOI 10.2108/zsj.29.672.
- Solà E, Álvarez-Presas M, Frías-López C, Littlewood DTJ, Rozas J, Riutort M. 2015. Evolutionary analysis of mitogenomes from parasitic and free-living flatworms. *PLOS ONE* 10:e0120081 DOI 10.1371/journal.pone.0120081.
- Song H, Buhay JE, Whiting MF, Crandall KA. 2008. Many species in one: DNA barcoding overestimates the number of species when nuclear mitochondrial pseudogenes are coamplified. *Proceedings of the National Academy of Sciences of the United States of America* 105:13468–13491 DOI 10.1073/pnas.0803076105.
- Stamatakis A. 2014. RAxML version 8: a tool for phylogenetic analysis and post-analysis of large phylogenies. *Bioinformatics* 30:1312–1313 DOI 10.1093/bioinformatics/btu033.
- Stimpson W. 1857. Prodröm descriptionis animalium evertibratorum, quae in expeditione ad oceanum Pacificum Septentrionalem, Johanne Rogers duce a Republica Federata missa, observavit e descriptit. *Proceedings of the Academy of Natural Sciences of Philadelphia* 1–5 DOI 10.5962/bhl.title.51447.
- von Graff L. 1896. Über das System und die geographische Verbreitung der Landplanarien. *Verhandlungen Deutsche Zoologische Gesellschaft* 6:75–93.
- von Graff L. 1899. *Monographie der Turbellarien. II. Tricladida, Terricola (Landplanarien)*. Leipzig: Englemann.
- Whitehouse RH. 1914. Land planarians. In: *Zoological Records of the Arbor Expedition 1911-1912 Part 3 No. 22*, Vol. 8. Records of the Indian Museum, 455–464.
- Winsor L. 1983. A revision of the Cosmopolitan land planarian *Bipalium kewense* Moseley, 1878 (Turbellaria: Tricladida: Terricola). *Zoological Journal of the Linnean Society* 79:61–100 DOI 10.1111/j.1096-3642.1983.tb01161.x.
- Winsor L. 1998a. Aspects of the taxonomy and functional histology in terrestrial flatworms (Tricladida: Terricola). *Pedobiologia* 42:412–432.
- Winsor L. 1998b. The role of the atrial diverticulum in the copulatory apparatus of the terrestrial flatworm *Platydemus manokwari* de Beauchamp (Tricladida: Terricola). *Hydrobiologia* 383:83–89 DOI 10.1023/A:1003451829795.
- Winsor L, Sluys R. 2018. Basic histological techniques for planarians. In: Rink JC, ed. *Planarian Regeneration Methods in Molecular Biology*. New York, NY: Humana Press, 285–351.
- Winsor L. 2003. Studies on the systematics and biogeography of terrestrial flatworms (Platyhelminthes: Tricladida: Terricola) of the Australian region. Ph. D. thesis. James Cook University, Townsville, Queensland.
- Yamamoto K. 2000. *Bipalium* sp. Kumamoto–1. *Junshin Chûgakkô-Junshin Joshi Kôtôgakkô Kiyô* 27:39–41 (In Japanese).